Investigating Carbon Sequestration in Cementitious Mortars with Low-Carbon Binders and Carbonated Water

Aswathy Rajendran*, Sripriya Rengaraju, Abir Al-Tabbaa

Department of Engineering, University of Cambridge, Cambridge CB2 1PZ, UK

**Corresponding author: ar2221@cam.ac.uk*

ABSTRACT

The use of carbonated water in cementitious systems as a carbon sequestration strategy is promising, offering operational simplicity and high CO_2 binding efficiency compared to approaches such as gaseous CO_2 injection and carbonation curing. However, its application in low-carbon cement systems, particularly emerging binders such as limestone calcined clay cement (LC^3), remains underexplored. As the shift to low-carbon binders is critical for reducing embodied carbon in cement, it is essential to understand their interactions with carbonated water, given their distinct reactivity, pH evolution, and fresh-state behaviour. This study systematically investigates the effects of carbonated water on conventional low-carbon binders (Slag-50% and Slag-80%), emerging LC^3, and OPC mortars. Evaluations covered fresh-state properties, mechanical performance, durability (sorptivity and porosity), and microstructural evolution at early and later ages. Results show the strongest interaction of carbonate ions with C_3A and its hydration products, with CO_2 binding governed by the nature of early hydrates and pH conditions. Contrary to the hypothesis that high-calcium systems such as OPC are most favourable for CO_2 binding, they exhibited reduced strength and durability. In contrast, LC^3 and Slag-50% demonstrated the greatest benefits, with improved CO_2 binding, shortened setting times, enhanced strength and reduced sorptivity and porosity. Microstructural analysis confirmed CO_2 binding predominantly influenced calcium-silicate-hydrate gels with minimal calcite formation. Overall, carbonated water emerges as a practical pathway to improve performance while enabling additional CO_2 binding in LC^3 and slag-50% cement systems, reinforcing their superior potential for carbon sequestration to OPC.

Keywords

Carbonated water; Low-carbon cement; pH; CO_2 binding

1. INTRODUCTION

Recent decarbonisation roadmaps for the construction industry project that Carbon Capture and Storage (CCS) and Carbon Capture and Utilisation (CCU) technologies could collectively contribute between 33% and 60% of the achievable emissions reductions in cement and concrete production (ECA roadmap; MPA roadmap). Despite the recognised importance of CCS, which involves capturing CO_2 from point sources such as cement kilns and storing it permanently underground, its large-scale implementation remains constrained by unresolved challenges, including the risks of CO_2 leakage and potential groundwater contamination (Celia, 2017; Zheng et al., 2021). These inherent limitations underscore the need to diversify carbon sequestration strategies within the sector, with increasing emphasis on CCU pathways that reuse captured CO_2 as a feedstock for producing value-added materials (Chang et al., 2024). Such approaches not only enhance process safety and carbon circularity but also generate both economic and environmental value through CO_2-integrated products. Among emerging CCU technologies, mineral carbonation, particularly within cementitious systems, represents one of the most promising routes for achieving permanent immobilisation of carbon. This approach sequesters carbon through an accelerated equivalent of natural rock weathering where CO_2 is converted into stable carbonate minerals, embedding carbon within the built environment and contributing to a closed carbon cycle.

Mineral carbonation primarily leverages calcium and magnesium-rich materials due to their high reactivity with CO_2. The thermodynamic stability of resulting carbonates, demonstrated by their substantially lower Gibbs free energy relative to CO_2, ensures long-term permanence of the sequestered carbon [Hanifa et al., 2023]. The fundamental reaction for mineral carbonation is summarised in Equation 1.

$$CaO/MgO + CO_2 \rightarrow CaCO_3/MgCO_3 + Heat \quad \text{Eq. (1)}$$

The unique suitability of cement for mineral carbonation stems from its chemistry dominated by Bogue compounds such as tricalcium silicate (C_3S), dicalcium silicate (C_2S) and tricalcium aluminate (C_3A), along with cement hydration products including calcium silicate hydrate (C-S-H) gel, portlandite (CH), and ettringite (AFt). These compounds and phases contain reactive calcium species capable of undergoing reactions with CO_2 to predominantly form thermodynamically stable calcite ($CaCO_3$), enabling effective CO_2 sequestration (Hanifa et al., 2023; Kashef-Haghighi et al., 2015; Kazemian and Shafei, 2023).

Among various mineralisation strategies in concrete, gaseous CO_2 injection and carbonation curing are the most widely studied. In gaseous injection, CO_2 in gaseous form is injected during mixing to dissolve in pore water and react with cement hydrates, while in carbonation curing, hardened concrete is exposed to concentrated CO_2 gas to accelerate surface mineralisation (Davolio et al., 2025; Han et al., 2025). However, the rapid formation of a dense calcite layer during curing limits further gas penetration, making mass transport the rate-limiting step; studies report only 14% of the theoretical CO_2 uptake is achieved due to this barrier (Stripple et al., 2018; Kashef-Haghighi and Ghoshal, 2010). Carbonation induced decalcification of hydration products can also degrade the material integrity and promote cracking (Ghantous et al., 2017), reinforcing perceptions of hardened-state carbonation as a deterioration mechanism rather than a viable sequestration route (Forsdyke and Lees, 2022; Galan et al., 2010).

In contrast, gaseous CO_2 injection enables direct gas-solid interactions, with CO_2 dissolving in mixing water and dissociating into carbonate (CO_3^{2-}) and bicarbonate (HCO_3^-) ions depending on system pH (De Weerdt et al., 2019). These ions facilitate mineral dissolution and carbonate precipitation, with commercial implementations such as CarbonCure technologies (Niven et al., 2016) demonstrating feasibility for uptake up to 5%.

An alternative and potentially superior approach to gaseous CO_2 injection is the use of carbonated water as mixing water, which supplies CO_2 directly in a pre-dissolved form, bypassing the kinetic limitations associated with the stepwise dissolution of gaseous CO_2. The immediate availability of dissolved CO_2 accelerates carbonation reactions, enhances CO_2 utilisation efficiency, and simplifies process integration compared to gaseous injection systems (Davolio et al., 2025). For these reasons, this study adopts carbonated water as the mixing water to serve as a CO_2 sequestration route. Beyond its technical advantages, the approach can also be seamlessly integrated into existing construction practices, offering an immediate and practical pathway toward net-zero concrete.

2. USE OF CARBONATED WATER IN CEMENTITIOUS MATERIALS: PRIOR STUDIES, GAPS AND RESEARCH RATIONALE

Research on carbonated water for carbon sequestration remains nascent, with only three studies: Kwasny et al., 2014, Dos Santos et al., 2019, and Suescum-Morales et al., 2022 reported to date. Kwasny et al. used carbonated water with a high concentration of 47 g/L CO_2, generated in a pressurised steel vessel, mixed with cement in a sealed chamber. In contrast, Suescum-Morales et al. employed commercial carbonated water with moderate concentration of 14 mg/L CO_2 with a pH of approximately 4.8, incorporating recycled aggregates to enhance carbonation potential. Santos et al. applied carbonated water to improve the physical and mechanical properties of fibre cement composite, using the lowest CO_2 concentration of dosage of 3.8-4.2mg/L. All these studies focused on OPC systems, with Suescum-Morales additionally examining the effects of recycled aggregates.

These studies primarily investigated the cement phases in which CO_2 was bound and their subsequent effects on strength and durability, with results varying considerably across the different investigations. For instance, Kwasny et al., 2014 observed a significant decrease in

hydration rate at higher CO_2 concentrations, attributed to carbonation products initially coating the cement particles. X-Ray diffraction (XRD) analysis confirmed this effect, revealing distinct phase differences compared to normal water mixes. In normal water mixes, phase peaks of gypsum, C_3A, C_3S, and C_2S decreased rapidly after the initial 25 minutes, indicating active hydration, whereas their slower reduction in carbonated water mixes reflects inhibition of early-phase dissolution and hydration. However, carbonated water mixes exhibited extensive needle-shaped structures, with energy dispersive X-ray spectroscopy (EDS) confirming significant CO_2 content. These structures are speculated to be ettringite with carbonate ions potentially substituting sulfate ions. Conversely, the moderate 14 mg/L CO_2 concentration study by Suescum-Morales et al., 2022 reported a 20% increase in compressive strength at one and seven days, except for normal aggregates, which showed reduced one-day strength due to impaired initial hydration from lower pH conditions. This study also noted increased porosity, reduced dry bulk density, and higher calcite peak intensity alongside a slight decrease in portlandite peak intensity at one day. Similarly, Santos et al., 2019 reported beneficial effects of carbonated water at lower CO_2 concentrations, concluding that carbonation during hydration improves matrix densification, enhances mechanical strength, and promotes early-age curing. The varying CO_2 concentrations used across these studies resulted in distinct microstructural and mechanical responses, reflecting differences in carbonation kinetics and phase evolution.

While the feasibility of using carbonated water in OPC systems has been demonstrated in these studies, its application to low-carbon cements remains largely unexplored. This gap limits understanding of its effectiveness across diverse supplementary cementitious materials (SCMs) and evolving cement chemistries. Low-carbon cements, characterised by lower cement content, reduced CaO levels, altered phase assemblages, and different hydration pathways, exhibit varied carbonation effects under diffused CO_2 exposure in hardened state carbonation (Von Greve-Dierfeld et al., 2020; Winnefeld et al., 2022). Consequently, these compositional

differences are also expected to influence their interaction with carbonated water, potentially resulting in variations in carbonation kinetics and efficiency. Such variations present an opportunity to synergistically couple cement reduction with enhanced carbon sequestration, offering a dual pathway to sustainability.

Unlike hardened-state sequestration which primarily involves carbonation of C-S-H compounds, portlandite, and ettringite, fresh-state carbonation via carbonated water is inherently more complex as it interacts directly with SCMs and the evolving hydration reactions. In OPC, CO_2-reactive phases include Bogue compounds, whereas in slag systems, both Bogue phases and periclase (MgO) contribute (Biava et al., 2024; Gao et al., 2024). In clay-based cement systems such as LC^3, metakaolin derived hydration products can bind CO_2 through the formation of stable carboaluminate phases via alumina-carbonate reactions (Li et al., 2025; Sun et al., 2024a). Hence, these differing CO_2 reactive phases of various cement systems, implies that carbonated water may suit certain cementitious systems better than others. Although reduced CaO content in high-SCM mixes may limit CO_2 binding (Gunning et al., 2010), the optimum cement content level where the benefits of CO_2 binding via carbonated water is maximised needs experimental verification.

Further, the low pH (~4-5) of carbonated water introduces additional complexity to the cement pore solution. While acidic conditions promote mineral dissolution and increase release of calcium ions (Suraneni 2015), higher pH values are required to stabilise carbonate ions critical for CO_2 binding (Aghaee, 2025). Hence, an optimal balance between pH, calcium availability, and carbonate stability is essential for effective CO_2 sequestration without compromising hydration. This challenge is particularly relevant in low-carbon systems, which inherently exhibit lower pore solution pH than OPC (García Calvo et al., 2013; Natkunarajah et al., 2022). Identifying suitable combinations of cement chemistry and carbonated water pH that enhance CO_2 uptake while maintaining hydration kinetics therefore remains a key research need.

To address these gaps, the present work systematically examines the use of carbonated water in both conventional OPC and low-carbon cement systems, focusing on the influence of solution chemistry, arising from pH changes and ion concentrations, on CO_2 binding and hydration mechanisms. Novel binders such as limestone calcined clay cement (LC^3) and conventional low-carbon slag systems are examined for the first time in this context. A multi-scale evaluation spanning fresh, hardened, and microstructural stages is undertaken to clarify how carbonated water affects CO_2 sequestration and material performance. The findings aim to guide industry in selecting cement formulations that maximise carbon sequestration while ensuring strength and durability, a critical but often overlooked consideration in sustainable sequestration practices.

3. MATERIALS USED

3.1 Cement

The cement types investigated in this study encompass a broad spectrum of Portland cement content, ranging from 100% to 20% (Figure 1). For the cement replacements, SCMs such as slag and calcined clay were employed. Slag was chosen for its potential to replace a high percentage of Portland cement, while calcined clay was included as a low-carbon alternative, especially given potential future restrictions on the availability of fly ash and slag. The cement types were carefully selected to ensure comparable strength development and microscopic structure, allowing for a fair comparison of carbonated water effects. Table 1 presents the elemental composition of OPC and the various SCMs. The diverse range of elemental compositions was selected to explore the interactions of carbonate ions with different elements and the resulting hydration products. Table 2 provides a detailed overview of the cement systems, including clinker percentages and SCM types and quantities. The calcined clay used in the LC^3 cement was produced by calcining raw kaolinite clay at approximately 800°C for

one hour in accordance with the recommendations of Scrivener et al., 2018 and the Bureau of Indian Standards code IS18189. Notably, the LC^3 system also includes limestone, comprising about 15% of the total cement content, as detailed in Table 2. No additional gypsum was added to the low-carbon cement mixes for optimisation. This approach was adopted to maximise potential CO_2 binding, as gypsum can compete with carbonate ions for calcium sites (Bonavetti et al., 2001). Moreover, the optimisation of gypsum content in low-carbon cements depends on multiple factors, including SCM surface area and alite reactivity (Zunino and Scrivener, 2022), and was therefore considered beyond the scope of this study.



***Figure 1**: Cement types explored in the study*

***Table 1**: Elemental composition of OPC and SCMs used in the study*

Chemical composition	OPC	Slag	Clay	Limestone
CaO	61	37.1	0.05	48.3
SiO_2	19.4	36.1	49.3	10.2
Al_2O_3	4.6	10.4	35.7	1.5
MgO	3.3	13.2	0.1	0.5
SO_3	2.3	3.4	0.11	0.01
Fe_2O_3	2.0	0.7	0.97	1.5
Na_2O	2.0	0.4	0.3	-
K_2O	0.7	0.5	0.4	0.1
LOI	1.4	2.5	9.2	35.4

***Table 2**: Cementitious systems explored in the study*

Cement types	Portland cement content (%)	Type of SCM	SCM %

OPC	100	NIL	0
Slag-50%	50	Slag	50
Slag-80%	20	Slag	80
LC^{3*}	50	Calcined clay	35

204 * The LC^3 mix further comprises of 15% limestone

205 Furthermore, the variation in hydration phases across different cement systems influences the
206 binding of CO_2 in the resulting hydration products. This is evident in the carbonation reaction
207 equations of these products, as reported in literatures (Kazemian and Shafei, 2023; You et al.,
208 2022). Accordingly, Table 3 presents the primary hydration phases anticipated in the cement
209 systems under investigation.

210 ***Table 3**: Hydration product phases in the cement systems used in the study (Kolani et al.,*
211 *2012; Sun et al., 2024)*

Cement Type	**Hydration products**	
	Dominant phases	**Minor phases**
OPC	Calcium silicate hydrate (C-S-H) Portlandite (CH)	Ettringite (AFt), monosulfate (AFm)
Slag cements	Calcium alumino silicate hydrate (C-A-S-H)	Calcium silicate hydrate (C-S-H) Portlandite (CH) Ettringite (AFt), monosulfate (AFm)
LC^3	Calcium alumino silicate hydrate (C-A-S-H) Mono and hemi carboaluminates (AFm) Ettringite (AFt)	Portlandite (CH)

212 **3.2 Mixing water**

213 Carbonated water containing approximately 6 g/L CO_2 and a pH range of 4.8 to 5.3 was
214 employed to facilitate mineral carbonation (Figure 2), with all cement mixes prepared using
215 both this carbonated water (CW) and normal tap water (NW) (pH ~7) as a control. To pertain
216 to the standard pH requirements of $\geq$4 for mixing water (BS EN 1008) and minimise adverse
217 effects such as reduced workability, increased permeability, and surface pore formation upon
218 gas escape linked to elevated CO_2 levels (Liang et al., 2024; Liu et al., 2021; Pham et al., 2024),

a CO_2 dosing of 0.3% by weight of cement was selected. Although the carbon savings associated with such a low dosage are minimal, substantial reductions can be achieved when applied at scale. Moreover, the primary objective of this study is to investigate dosage levels that not only sequester CO_2 but also impart beneficial effects on strength and durability. This rationale is supported by findings from three previous studies on the use of carbonated water (Kwasny et al., 2014), (Dos Santos et al., 2019), (Suescum-Morales et al., 2022), where lower dosages demonstrated potential improvements in performance, thereby motivating the selection of 0.3% CO_2 for the present work. A fresh bottle of carbonated water was used for each mix to limit CO_2 loss from gas escape. Importantly, pH loss of carbonated water was minimal, with only a 4% decrease observed after 30 minutes, indicating that this combination of CO_2 concentration and pH stability is reasonable for potential large-scale application where the mixture can be used within 30 minutes of opening the carbonated water storage vessel.

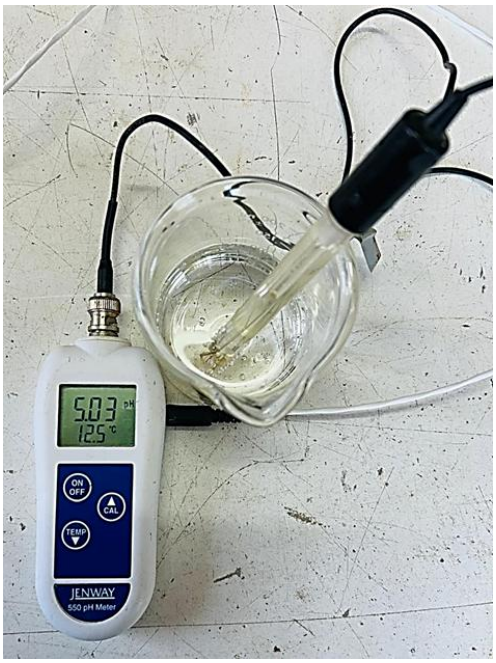


Figure 2: *Carbonated water used for the study (pH 4.8 to 5.3)*

3.3 Fine aggregate

In this study, fine aggregate conforming to the specifications of BS EN 13139 was used, with a particle size passing through a 4.75 mm sieve.

4. MORTAR MIX PROPORTION AND FABRICATION

All mortars were cast with a constant water-to-cement (w/c) ratio of 0.5 and a cement-to-sand (c/s) ratio of 1:3. The specific mix proportions for 1 kg of dry mortar are detailed in Table 4. To ensure a workable consistency, a high-range water-reducing admixture (Sikament LA45), characterised by normal set behaviour and minimal retarding effect, was incorporated into the mortar mixture. The mortar was prepared in a 10-liter Hobart mixer by first dry-mixing the cement and sand, followed by the gradual addition of carbonated or normal water and the admixture. The admixture dosage was determined to achieve a flow table value (described in Section 5.1) within the range of 160-230 mm, representing a workable consistency for all cement systems investigated in this study. After achieving the desired workability, the fresh mortar was cast into moulds and sealed for 24 hours to prevent premature moisture loss. The specimens were then demoulded and subjected to a 28-day water-curing process using normal water. The curing setup involved a box-shaped container filled with water-saturated gravel to a depth of approximately 40 mm (as shown in supplementary data S1) maintained at approximately 20 ºC. A perforated base plate was positioned atop the gravel to support the specimens. This setup ensured consistent moisture conditions without excessive water exposure to the specimens, minimising potential leaching effects.

Table 4: *Mix proportions of mortar mixes for 1 kg of dry mortar*

Mix-ID	w/c	Weight (gms)			Admixture % (by wt. of cement)
		Cement	SCM	Sand	
OPC - NW	0.5	250	-	750	0.61
OPC - CW	0.5	250	-	750	0.62
Slag 50% - NW	0.5	125	125	750	0.54
Slag 50% - CW	0.5	125	125	750	0.54
Slag 80% - NW	0.5	50	200	750	0.54
Slag 80% - CW	0.5	50	200	750	0.56

LC^3 - NW	0.5	125	125*	750	2.35
LC^3 - CW	0.5	125	125*	750	2.41

* 87.5gm: Calcined clay; 37.5gm: Limestone

5. TEST METHODS

5.1 Fresh state properties

To comprehensively characterise fresh state properties, four key tests were conducted: workability assessment using flow table on mortars, and pH measurement, setting time determination, and early-age hydration monitoring via isothermal calorimetry on cement paste. For cement paste tests, compositions corresponding to that of Table 4 without admixtures were used. The flow table test followed BS EN 1015-3 by measuring the spread diameter of the mortar after 15 jolts (see supplementary S2). The pH measurement evaluated the effect of carbonated water by preparing paste samples with normal and carbonated water at consistent w/c ratios, centrifuging approximately 30 mL of paste for 7 minutes (see S3), then measuring the pH of the extracted clear water using a calibrated pH meter, with calibration performed at least one day prior to testing. Initial and final setting times were determined using Vicat apparatus as per ASTM C191 to examine CO_2 binding effect on setting properties of the mixes. Early-age hydration was monitored using an 8000HPC isothermal calorimeter on sealed paste samples prepared by mixing 25 g of cement with 25 g of water. The samples were placed in the calorimeter maintained at a constant temperature of 20 ºC to monitor heat evolution under stable thermal conditions. Hydration was recorded continuously for up to 3 days until the hydration curves stabilised (see S4).

5.2 Hardened state properties

To assess the hardened state properties and the impact of CO_2 binding, compressive strength, sorptivity, and porosity tests were performed. Compressive strength was measured on 40 mm

mortar cubes as per BS EN 1015-11 at 1, 7, 28, and 56 days, ensuring specimens were surface-dry before testing for consistency. Early strength (1 day) indicated initial setting behavior, while strengths at 28 and 56 days evaluated sustained effects of CO_2 binding on strength development. Durability-related properties were assessed at 28 days via sorptivity as per ASTM C1585 to quantify capillary water absorption, measured by mass gain over time on one exposed specimen face (see S5). Sorptivity was calculated from the slope of cumulative absorbed water per unit area against square root of time, reflecting pore structure and water penetration resistance. Indicative porosity was estimated following the University of Cape Town durability index manual, by calculating percentage differences between saturated and oven-dry specimen weights, representing pore volume relevant to durability.

5.3 Microstructural studies

Microstructural investigations comprising of thermogravimetric analysis (TGA) and XRD were conducted at 7 days to provide insight into the phase assemblages formed and modified due to CO_2 binding within the system. This time point was chosen to understand the early mechanisms by which CO_2 influences cement hydration and development, as differences induced by carbonated water may tend to stabilise at later ages. Cement pastes prepared for microstructural analysis maintained the same w/c ratio as the mortar mixes and excluded any chemical admixtures. Sample preparation involved crushing the paste specimens after 7 days of curing, followed by further grinding to achieve a particle size fine enough to pass through a 75 μm sieve. Hydration of these fine powders was then stopped using the solvent exchange method described in Scrivener et al., 2018, whereby approximately 3 grams of powder were immersed in isopropanol for 10 minutes, vacuum filtered with two additional isopropanol washes and one diethyl ether wash, then dried at 40ºC for 10 minutes before storage in a desiccator until analysis. XRD analysis was conducted using a Siemens D500/501 Diffractometer to identify the mineral phases present in the paste powder samples. Copper K-

alpha radiation was employed with power settings of 40 kV and 20 mA. XRD patterns were collected over a 2θ range of 2° to 70° with a step size of 0.02° and a scan time of one second per step. For TGA analysis, approximately 15-20 mg of powdered sample was placed in an alumina crucible under an argon gas atmosphere. The temperature was ramped from 30 °C to 950 °C at 10 °C/min, held isothermally for 1 minute at 950 °C, then cooled back to 30 °C at the same rate of 10 °C/min. The thermal decomposition and dehydration processes of the cement phases present in the powder, such as portlandite, calcite, and amorphous hydrates, were indicated by mass losses observed in the thermogravimetric and differential mass loss curves. These curves were used to identify the mass loss of each critical phase, as the temperature at which these processes occur is typical for the mineral or hydrate. The mass loss occurring within specific ranges was recorded for normal and carbonated water samples of each cement type, and the approximate quantification of these phases was conducted using the method described in Scrivener et al., 2018.

6. TEST RESULTS AND DISCUSSIONS

6.1 Fresh state properties

6.1.1 Workability

The workability results of the mortar systems, measured using the flow table method, are presented in Table 5 alongside the corresponding admixture dosages. A consistent decrease in flow was observed across all cement types when carbonated water replaced normal water, with reductions of 5-20%. This trend aligns with similar study by Monkman et al., 2016, who investigated the use of liquid CO_2 during mixing as an accelerating agent in concrete and observed a similar decrease in workability.

Table 5: *Fresh state properties of the mortar mixes*

Mix ID	Admixture dosage % (by weight of cement)	Flow (mm)
OPC – NW	0.6	165 × 170
OPC – CW	0.6	160 × 160
Slag – 50% NW	0.5	230 × 235
Slag – 50% CW	0.5	190 × 190
Slag – 80% NW	0.5	195 × 200
Slag – 80% CW	0.5	180 × 185
LC^3 – NW	2.3	175 × 185
LC^3 - CW	2.4	175 × 175

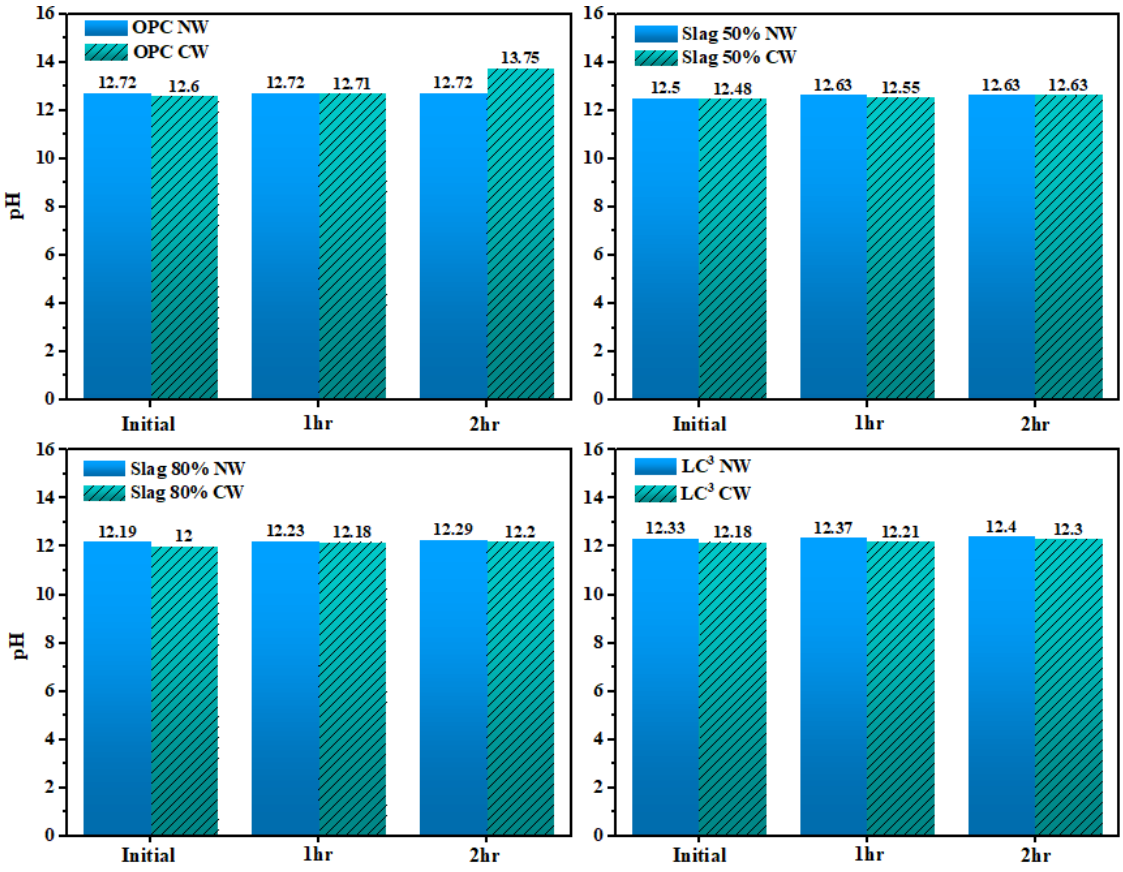
The reduced flowability in such CO_2 bound system has been mainly attributed to two factors: (i) accelerated C_3A hydration, leading to greater needle-shaped ettringite formation and increased mix viscosity (Jakob et al., 2019; Winnefeld et al., 2019), and (ii) the formation of nano-calcite phases with high surface areas that reduce fluidity (Cao et al., 2019; Syamsunur et al., 2022). Moreover, the transient disordered calcium hydroxide particles react with carbonate ions to form calcium carbonate polymorphs which serve as nucleation sites, facilitating the acceleration of the curing process (Kim et al., 2023; Stefaniuk et al., 2023).

Despite these effects, the admixture demand to achieve the target workability (160-230 mm) remained similar for most systems, about 1% by weight of cement. The LC^3 mix required a higher dosage (~3%) due to the high water retention of clays (Ferrari et al., 2024; Moghul et al., 2025). Overall, the reduction in workability remained within acceptable limits, indicating that the use of 0.3% CO_2 in mixing water does not significantly impair fresh-state performance.

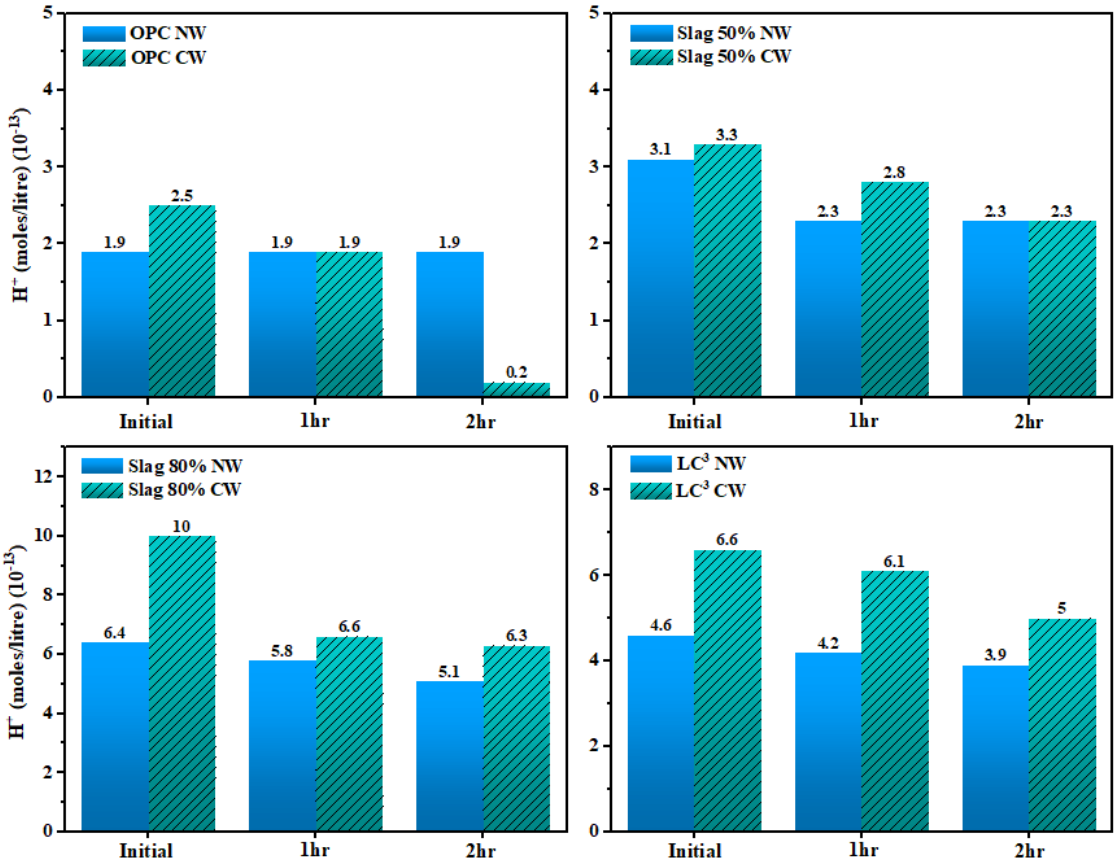
6.1.2 pH of paste

A potential drawback of using carbonated water in cement systems is the reduction in alkalinity. To assess this effect, the pH evolution of cement pastes prepared with normal and

carbonated water was monitored for two hours after mixing (Figure 3a), with the corresponding variation in H^+ concentration shown in Figure 3b. Beyond two hours, pH values for all systems stabilized, and subsequent measurements at 7 and 28 days revealed no significant differences between the two mixing waters. Consequently, the initial pH stabilisation period of approximately 2 hours, where a transient variation in pH was detected, is reported and discussed in this study.



(a) pH



(b) H^+ (moles/litre) (10^{-13})

Figure 3: *Evolution of (a) pH and (b) H^+ concentration over time in different cement types with normal and carbonated water*

The pH profiles (Figure 3a) show an initial decrease for all cement mixtures with carbonated water, which stabilises after approximately two hours. For low-carbon cements (slag and LC^3), the final pH converges with that of the normal water mixtures, whereas OPC maintains a slightly higher pH. These pH results are largely consistent with previous studies (Rashid and Singh, 2023), where the addition of gaseous CO_2 (up to 0.2% by weight of cement) resulted in either constant or marginal increases in pH, typically not exceeding 2%, across varying dosages. The initial pH reduction observed in this study is attributed to rapid binding of carbonate ions with calcium, consuming hydroxide ions and lowering solution alkalinity. This differs from gaseous CO_2 addition reported in Rashid and Singh, 2023, where slower gaseous dissolution and buffering by hydration products maintain near-constant pH. The enhanced

reactivity of dissolved CO_2 in carbonated water thus offers potential for improved CO_2 uptake during early hydration.

A lower initial pH increases H^+ concentration, which can promote calcium leaching from minerals such as C_3S and portlandite (Suraneni 2015; Tompkins et al., 2025). However, higher pH levels are more favorable for carbonate precipitation (Biava et al., 2024; Ramli et al., 2021). In this context, the modest pH variations seen here suggest distinct behaviors among cements: slag 80% and LC^3 systems, with slightly lower pH, may favor enhanced CO_2 binding, while OPC, with a more alkaline matrix, may promote calcite formation.

As shown in Figure 3b, corresponding H^+ concentration changes reflect this trend-decreasing by ~90% for OPC and increasing by 23-26% for slag 80% and LC^3 mixtures when mixed with carbonated water. These shifts may influence early hydration kinetics through modified dissolution behavior, the influence of which is further explored in Section 6.1.4, where the role of carbonate ions in the hydration processes of different cement systems is discussed. Further quantitative validation through calcium concentration measurements (e.g., Inductively coupled plasma - ICP analysis) is proposed for future work.

6.1.3 Setting times

The initial and final setting times of the cement pastes are summarised in Table 6. Carbonated water primarily reduced initial setting times, with the most pronounced effects in LC3 (25% reduction) and Slag 80% (18% reduction). OPC and Slag 50% showed minimal or no change. This trend aligns with studies using CO_2 during mixing (Davolio et al., 2025; Monkman et al., 2016; Rashid and Singh, 2023), though it differs from Wang et al., 2024, who reported greater OPC setting time reductions attributed to temperature rises from pressurised CO_2 gas compression rather than enhanced CO_2 reactivity.

The enhanced response in LC^3 and Slag 80% likely relates to their formation of monosulfate and carboaluminate phases (Table 3), which exhibit high CO_2 reactivity as reported in literature (Von Greve-Dierfeld et al., 2020; Zhang and Çopuroğlu, 2022). Although slag-rich systems typically show delayed setting, carbonated water appears to accelerate this process. Overall, the observed reductions in setting times, while noteworthy, are not severe enough to hinder the practical application of these cement formulations.

Table 6: *Initial and final setting time of cement pastes explored in this study*

Cement	Setting time	NW	CW
OPC	IST	70	65
	FST	220	220
Slag 50%	IST	90	90
	FST	270	265
Slag 80%	IST	110	90
	FST	300	295
LC^3	IST	60	45
	FST	265	257

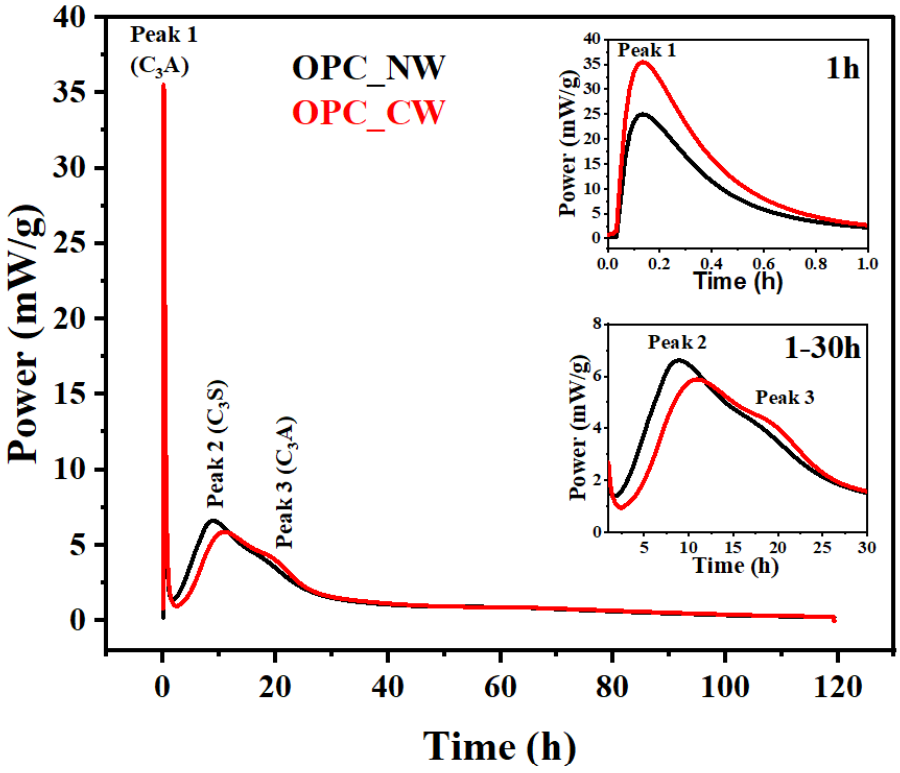
IST: Initial setting time; FST: Final setting time

6.1.4 Isothermal calorimetry

Isothermal calorimetry results (Figures 4-7), recorded at 0.3 J/s accuracy, show heat flow evolution during cement hydration. Peak 1 represents the initial C_3A + gypsum reaction forming ettringite, followed by an induction period that maintains paste workability. Peak 2 corresponds to the primary hydration C_3S reaction forming C-S-H, while Peak 3 reflects secondary C_3A hydration (Bhandari et al., 2023; Chen et al., 2025). In OPC, these secondary aluminate peaks typically appear as shoulder peaks to the major silicate hydration peaks. However, in low-carbon cements with elevated aluminate content, these peaks are observed to be more pronounced and dominant compared to the silicate peaks (Wang et al., 2022; Zunino and Scrivener, 2025). Subplots in Figures 4-7 display both 1-hour and 30-hour curves to clearly

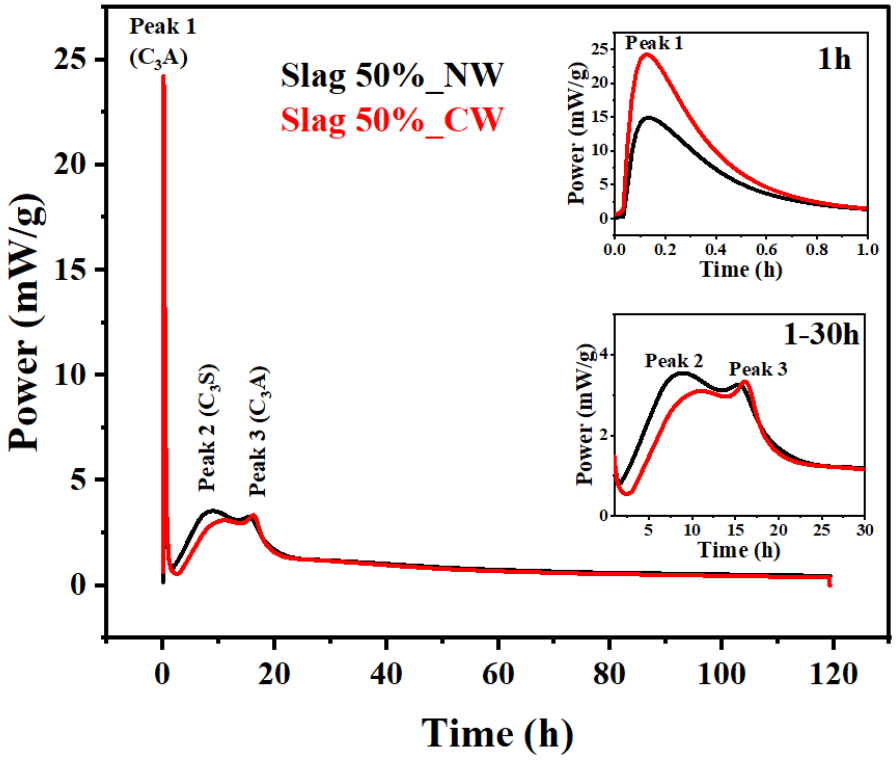
distinguish carbonated water effects on primary versus secondary hydration peaks across all systems.

Isothermal calorimetry results reveal that carbonated water consistently accelerates the reaction rates of C_3A phases (both the initial and secondary peaks) across all cement types, while retarding C_3S hydration in OPC and in the OPC fraction present in slag-50% systems. In OPC (Figure 4), the initial C_3A peak increases by 40%, whereas the C_3S peak is delayed by approximately 3 hours; the secondary C_3A peak shows a modest increase of ~10%. Similar behaviour is observed in slag-50% mixes (Figure 5), with a 38% rise in the initial C_3A peak, a 4% increase in the secondary peak, and a comparable delay in C_3S hydration. LC^3 systems (Figure 6) display the most pronounced changes, with a 78% increase in the initial C_3A peak and a 10% increase in the secondary peak. Slag-80% mixes (Figure 7) show a 50% rise in the initial C_3A peak and a modest 4% increase in the secondary peak. Notably, the secondary C_3A peak (Peak 3) occurs earlier in LC^3 and slag-80% systems (10-12 h) compared to OPC and slag-50% (19-20 h). These trends suggest that carbonate ions preferentially interact with aluminates, accelerating C_3A hydration, particularly in systems where early aluminate reactivity dominates (LC^3, slag-80%). A similar effect was reported in a study where CO_2 was introduced during mixing in a 3D-printed cementitious system, leading to accelerated hydration of C_3A (Li et al., 2023). However, the relatively low gypsum content in these binders would have further amplified this effect, as it would have also contributed positively to a more pronounced C_3A hydration effect in these systems.



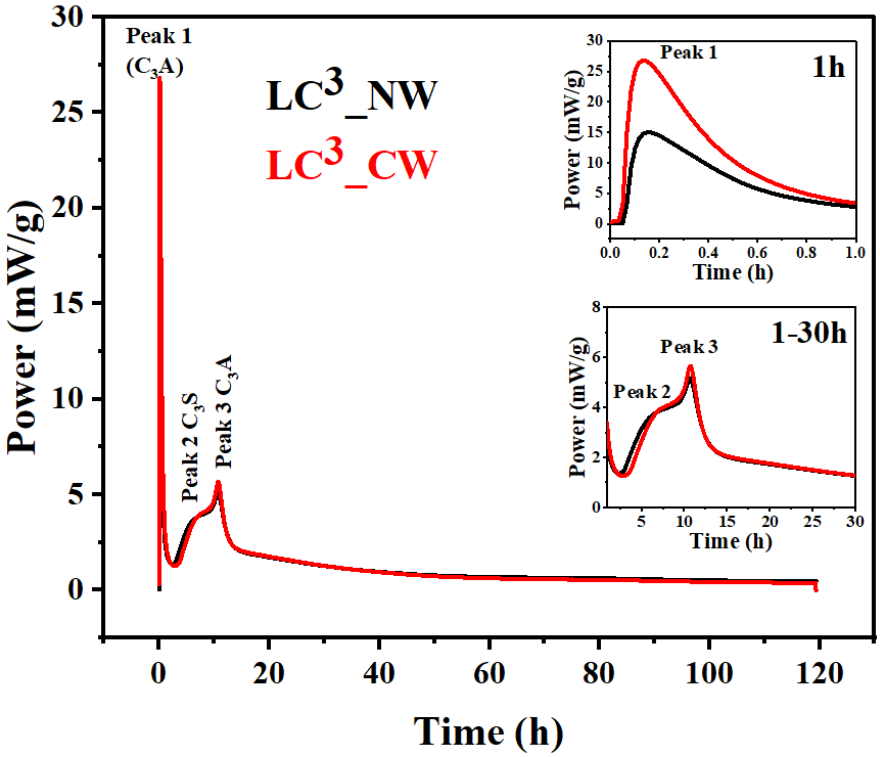
426

427 ***Figure 4:*** *Heat of hydration curves of OPC pastes with normal and carbonated water*



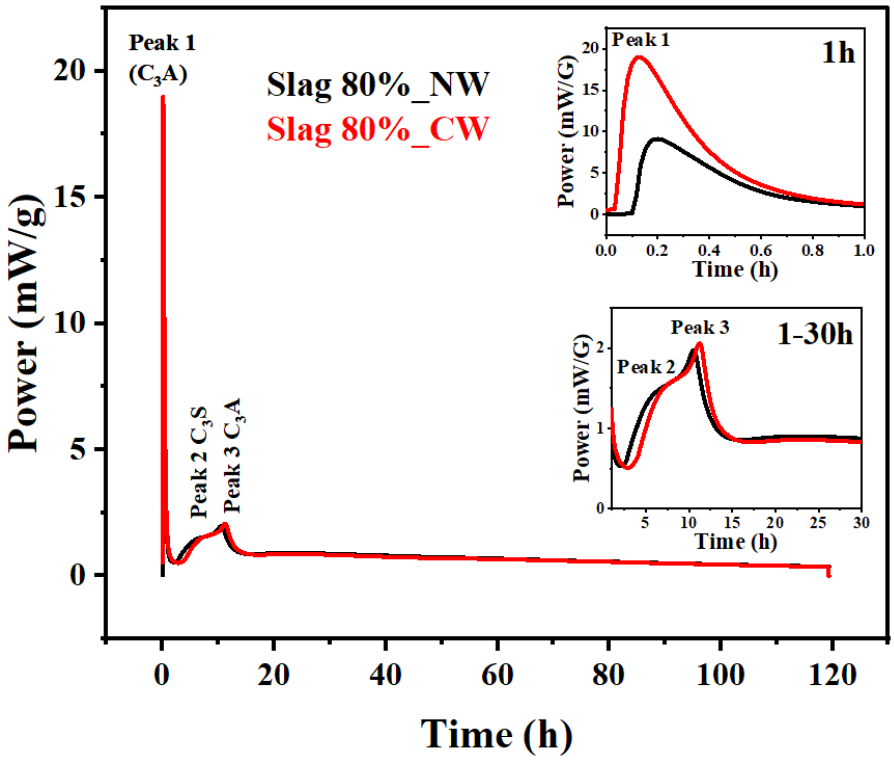
428

429 ***Figure 5:*** *Heat of hydration curves of Slag 50% pastes with normal and carbonated water*



430

431 ***Figure 6:*** *Heat of hydration curves of LC^3 pastes with normal and carbonated water*



432

433 ***Figure 7:*** *Heat of hydration curves of Slag 80% pastes with normal and carbonated water*

434 These peak alterations are further reflected in the cumulative heat evolution values, obtained

435 by integrating the calorimeter power curves. This data, summarised for the first 24 and 40 hours

in both absolute terms and relative percentages compared to normal water (NW) mixes, is presented in Figure 8, with percentage increases and decreases with respect to the NW mixes indicated directly on the figure. Results indicate that the heat of hydration decreases by 2-8% in OPC and slag-50% mixes, whereas it increases by 4-10% in LC^3 and slag-80% systems. These findings suggest that carbonated water enhances the overall early hydration in LC^3 and high-slag cements while impairing it in OPC and slag-50% systems. The cumulative heat flow values may also elucidate trends in early strength development, which will be further discussed in Section 6.2.1.

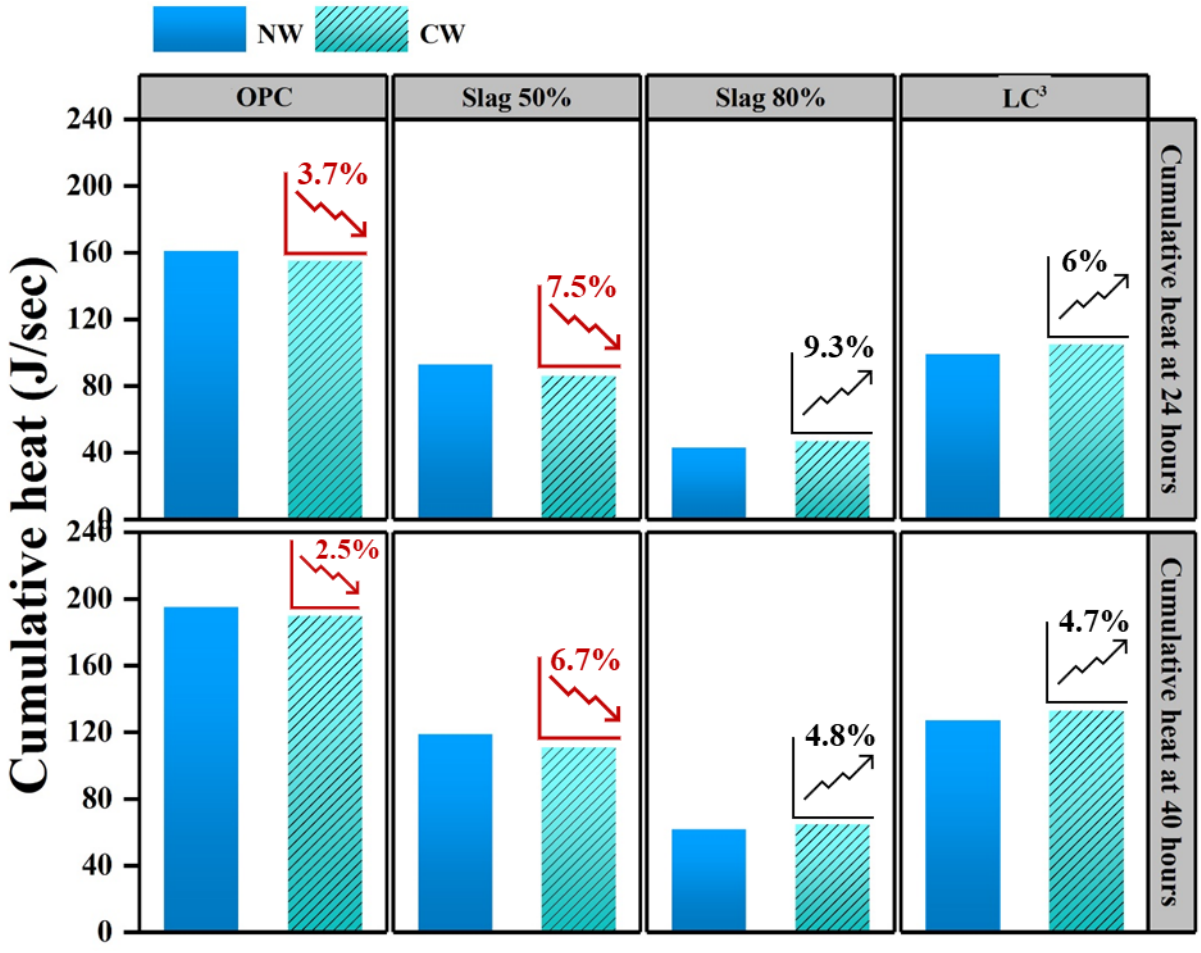


Figure 8: *Cumulative heat flow values of various cement systems at 24 and 40 hours of hydration under the influence of normal and carbonated water*

Similar effects of delayed C_3S hydration in OPC due to carbonation have been previously reported by Suescum-Morales et al., 2022, where carbonation products coating cement

particles delay initial C_3S hydration. This mechanism extends to slag-50% systems, which exhibit comparable hydration delays. In contrast, LC^3 systems show earlier hydration peaks (as observed with the secondary C_3A peaks here) compared to OPC, driven by the rapid reactivity of metakaolin and limestone components (Humagain et al., 2025). This accelerated early reaction likely mitigates the delaying impact of carbonated water on the main C_3S hydration peak. Although similar early secondary C_3A peaks were observed in slag-80% mixes, the lack of retardation in C_3S hydration is more reasonably attributed to their relatively lower C_3A content, resulting in fewer carbonation products forming coatings that impede C_3S hydration.

The observed alterations in the hydration peaks suggest that CO_2 ions may be incorporated into ettringite (calcium sulfoaluminate) formed during the initial C_3A peak (Peak 1), and into monosulfoaluminate phases formed during the subsequent C_3A peak (Peak 3). Previous studies (Carlson and Berman, 1960) on C_3A reactions with carbonate ions indicate theoretical molar ratios of CO_3^{2-} to C_3A about 0.33 (3 moles of C_3A with 1 mole of carbonate ions) for stable carboaluminate formation. At 0.3% CO_2 by weight of cement with typical 10 wt% C_3A, the calculated C_SA: CO_3^{2-} molar ratio is about 0.18 which means that all carbonate ions can be bound as monocarboaluminates without destabilising C_3A. Consequently, cement systems such as LC^3, characterised by higher reactive alumina content, have greater potential to bind CO_2 through these reaction products. This interpretation is supported by Srivastava et al., 2021 who reported significant carbonation in calcium sulfoaluminate cements with high aluminate content, and Sharma et al., 2023, who highlighted the pivotal role of ettringite in carbonation and its transformation into various crystalline forms of calcite.

To decipher the effects of carbonated water on accelerating C_3A hydration in low-carbon cement systems while retarding C_3S hydration in OPC, the influence of H^+ and OH^- concentrations on mineral dissolution was examined. It is well-established that increased H^+ concentration enhances mineral dissolution in cement systems (Juilland et al., 2010; Zhuang et

al., 2022). The pH results from section 6.1.2 show a 90% reduction in H^+ concentration in OPC with carbonated water after 2 hours, whereas LC^3 and Slag-80% cements exhibit a 25% increase. The elevated H^+ concentration in low-carbon systems likely promotes greater C_3A hydration, whereas the large decrease in OPC correlates with smaller increases in C_3A hydration.

The retarding effect on OPC C_3S hydration is further explained by the kinetics model of C_3S hydration by Damidot et al., 2007, where C_3S dissolution is positively influenced by H^+ concentration and negatively by $Ca(OH)_2$ concentration (Eq. 12).

$$\frac{dC_3S}{dt}\ (mmol/s\ m^2) = A.K_0.(SI-1)\ .[H^+]^{0.29}\ [CaOH^+]^{-0.27} \qquad \text{Eq. (12)}$$

The marked decrease in H^+ in OPC due to carbonated water likely hinders C_3S dissolution, whereas the slight H^+ increase in low-carbon systems mitigates retardation or even marginally enhances hydration. Regarding OH^-, low-carbon systems show ~20% decrease while OPC exhibits a substantial increase; a reduction in OH^- and thus $Ca(OH)_2$ further facilitates C_3S dissolution in LC^3 and slag-80%. This explains why these systems show no delay in C_3S hydration under carbonated conditions. Zhang et al., 2024 report similar findings in steel slag powders subjected to wet carbonation. Moreover, carbonation of ettringite, product of C_3A hydration, releases water that may enhance subsequent C_3S hydration. Systems with accelerated C_3A hydration under carbonated water, such as LC^3 and slag-80%, benefit from this additional water, which helps prevent hydration delays. It is also noteworthy that alkalis can affect the initial undersaturation of C_3S, reducing its dissolution (Wagner et al., 2023). Since sodium bicarbonate was present in the carbonated water used, its effect may have contributed to C_3S hydration delays observed in some systems. Though the exact sodium bicarbonate content is unknown, its possible influence should be considered.

6.2 Hardened state properties

6.2.1 Compressive strength

The compressive strength of the various mortar systems was evaluated at 1, 7, 28, and 56 days of curing. The strength results align closely with the hydration trends, showing modest increases in mortars where C_3A hydration is accelerated and decreases in systems where the pH trend led to lower H^+ concentrations, thereby reducing C_3S dissolution. Specifically, the compressive strength plot (Figure 9) shows a slight reduction in OPC systems at all ages, whereas slag-50% and LC^3 cement systems exhibit strength gains of 1-6 MPa at later ages. The highest increase was observed in LC^3 systems, with about a 12% strength enhancement in carbonated mixes compared to normal water mixes. In slag-80% systems, strength increased slightly at early ages (1 and 7 days) but decreased by approximately 2 MPa at later ages.

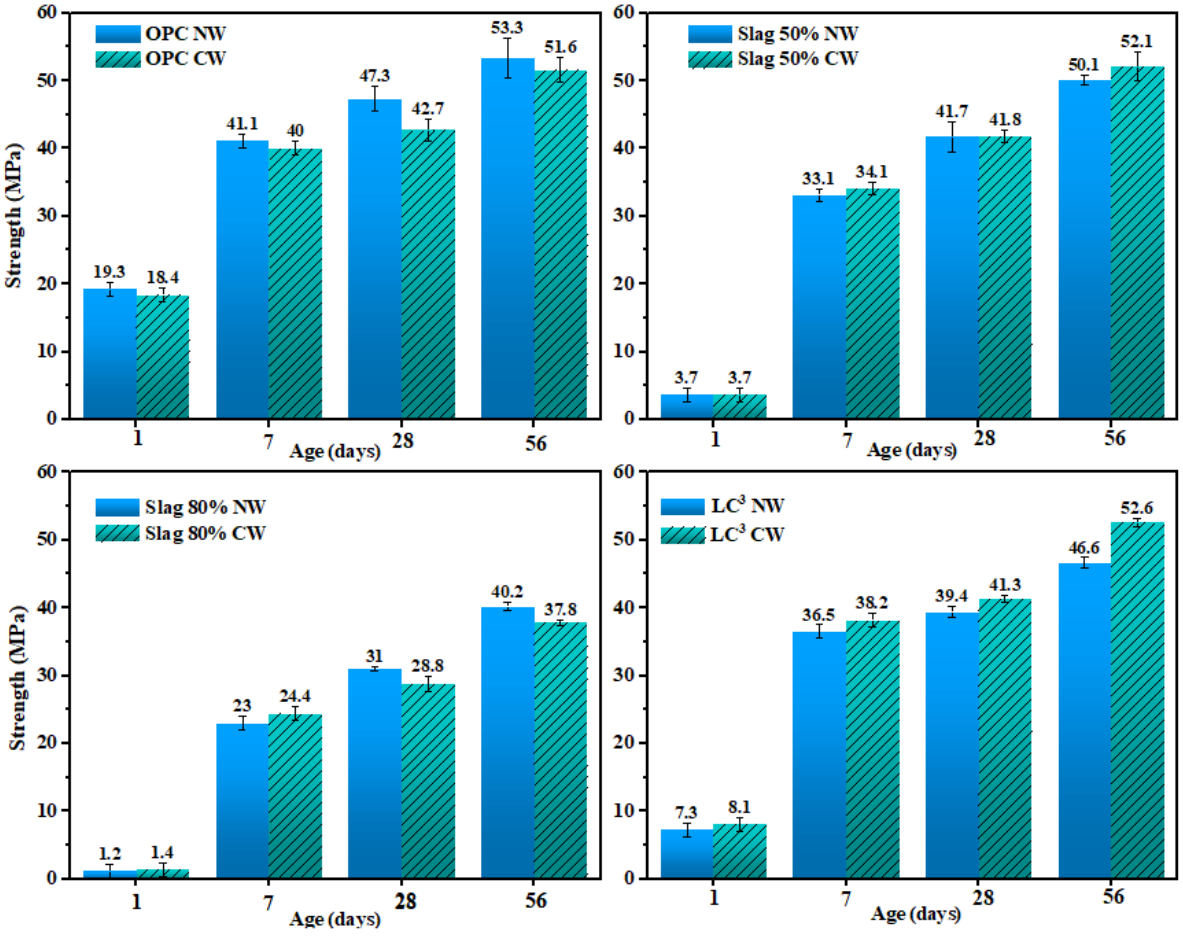


***Figure 9*:** *Compressive strength plot of the various cement systems with normal and carbonated water*

The enhanced early strength gain in low-carbon cements correlates with accelerated C_3A hydration observed in calorimetry results, consistent with literature reports (Winnefeld et al., 2019). Nano-calcite nucleation from carbonate-calcium interactions accelerates C_3A reaction rates (Monkman et al., 2016; Rashid and Singh, 2023). This is because these nano-calcites, much finer than C_3A, surround the C_3A particles. Upon contact with water, C_3A reacts with calcite to form carboaluminate layers, which are less permeable to water than ettringite. The continuous formation of such carboaluminate hydrates, characterised by large hexagonal plates, further promotes diffusion of water and sulfates through the C_3A surface, facilitating ettringite formation (Ramachandran and Chun-Mei, 1986). Additionally, crystalline ettringite formation fills pores and contributes to matrix densification, thereby enhancing strength (Scrivener et al., 2015). The conversion of ettringite to monosulfate has been reported to be delayed in the presence of carbonate ions due to sulfate-carbonate ion exchange (Bonavetti et al., 2001). In the presence of gypsum, C_3A reacts preferentially with sulfate to form ettringite (AFt), which can bind carbonate ions to produce less stable ettringite-carbonate phases. In contrast, without gypsum, carbonate ions directly react with C_3A hydration products to form more thermodynamically stable monocarboaluminates. The resulting monocarbonate phases are more stable than monosulfates, contributing to more durable microstructures (Holmes et al., 2022). Also, gypsum particles inhibit Ca^{2+} and CO_3^{2-} ion binding, directly lowering precipitation efficiency as noted in a study by J. Kim et al., 2023 exploring enzyme-induced carbonate precipitation.

Aluminates in SCMs can react with carbonate ions, as reported in low-carbon cement blends such as LC^3, where aluminates from SCMs interact with carbonate ions introduced via carbonated water to form carbonate-aluminate phases like monocarbonates. This aluminate-

carbonate reaction enhances later strength development by forming stable cementitious hydration products such as calcium carboaluminates and refining the microstructure (Li et al., 2025; Sun et al., 2024). In terms of the loss of strength in OPC, in addition to the pH and H^+ effects that hinder C_3S hydration discussed earlier, the higher C_3A content in OPC systems likely leads to increased formation of carbonation products, which may exert a stronger coating effect, delaying hydration (Zajac et al., 2022).

Earlier studies (Monkman et al., 2016; Rashid and Singh, 2023) on OPC systems that used CO_2 injection during mixing mostly found that adding CO_2 increased the strength. Motivated by these findings, higher CO_2 dosages were further investigated by adding sodium bicarbonate ($NaHCO_3$) at varying concentrations to OPC paste samples (supplementary data S6), revealing that a 10% $NaHCO_3$ dosage (equivalent to 5-10% CO_2) similarly enhanced hydration of both C_3A and C_3S phases, analogous to low-carbon cements. This enhancement likely results from increased carbonate ions reacting with free Ca^{2+}, improving ionic mobility as reported in a study by Ren et al., 2024, where lime mud was used as the source of carbonate ions. These findings suggest an optimal CO_2 dosage may exist, where low concentrations (<5%) cause coating-induced delays while higher dosages (>5%) promote hydration through enhanced solution chemistry.

Thus, from the evolution of strength results, it can be inferred that early CO_2 interaction with C_3A effectively accelerates strengths at all ages when the cement content is around 50%, as in LC^3 and slag-50% systems. Interestingly, calcium-aluminate and calcium-sulfate hydration products formed in carbonated water slightly increase strength in low-carbon cements, despite reports that carbonation of ettringite (calcium sulfoaluminate based) can reduce volume, increase permeability, and cause strength loss (Moffatt and Thomas, 2019). Further research is needed before generalising these observations; however, these findings highlight the potential for nucleation effects to outweigh strength losses in systems with approximately 50% clinker

replacement. However, the reduction in later age strength in slag-80% warrants further microstructural investigations to understand the specific hydration products formed in the presence of carbonate ions and their influence on later microstructure and mechanical performance.

6.2.2 Sorptivity and porosity results

The results of the sorptivity and porosity tests performed at 28 days are illustrated in Figures 10 and 11, respectively. The sorptivity and porosity results align well with the later-age compressive strengths, with OPC systems exhibiting an approximately 68% increase in sorptivity, whereas all low-carbon cements show reductions, the highest being 28% for slag 50% and 3-6% for slag 80% and LC^3. Porosity measurements follow these trends, with OPC showing a 10% increase and low-carbon cements demonstrating an 8-12% decrease.

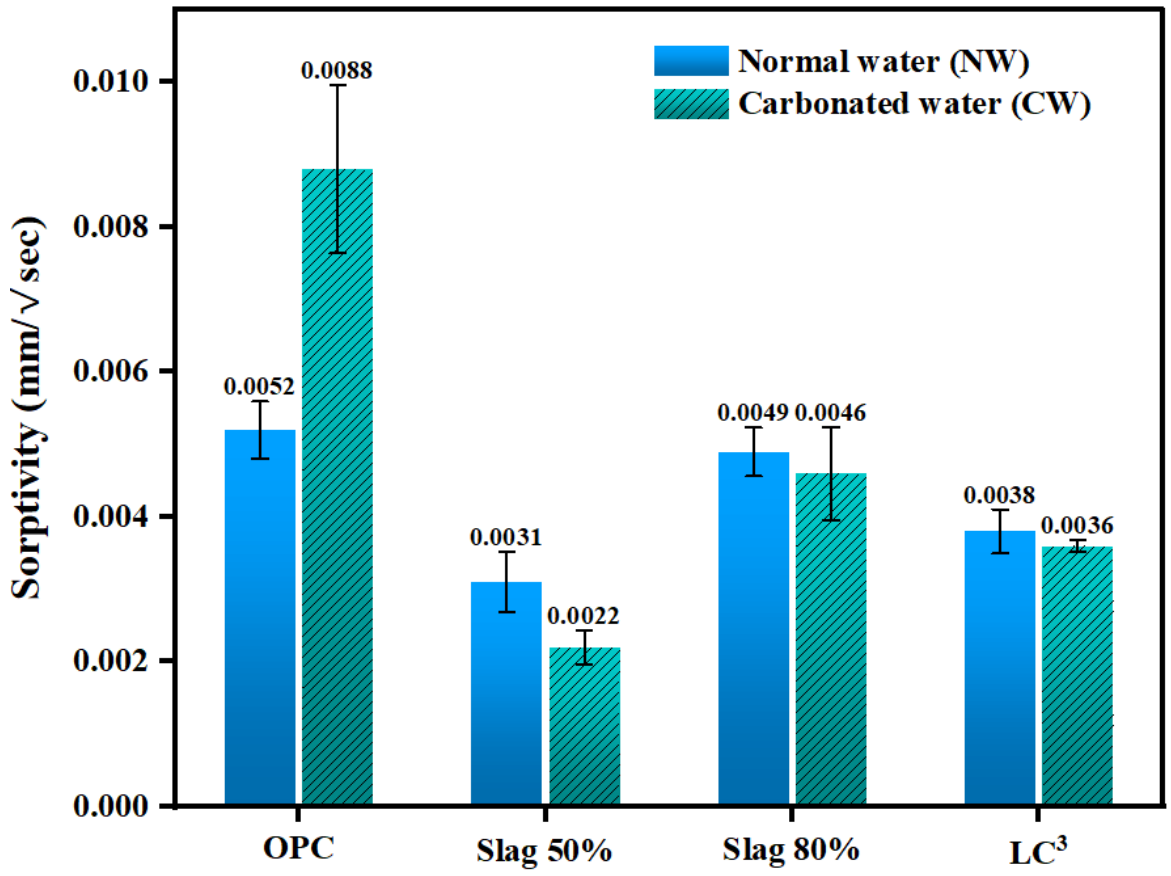


***Figure 10**: Sorptivity plot of the various cement systems with normal and carbonated water*

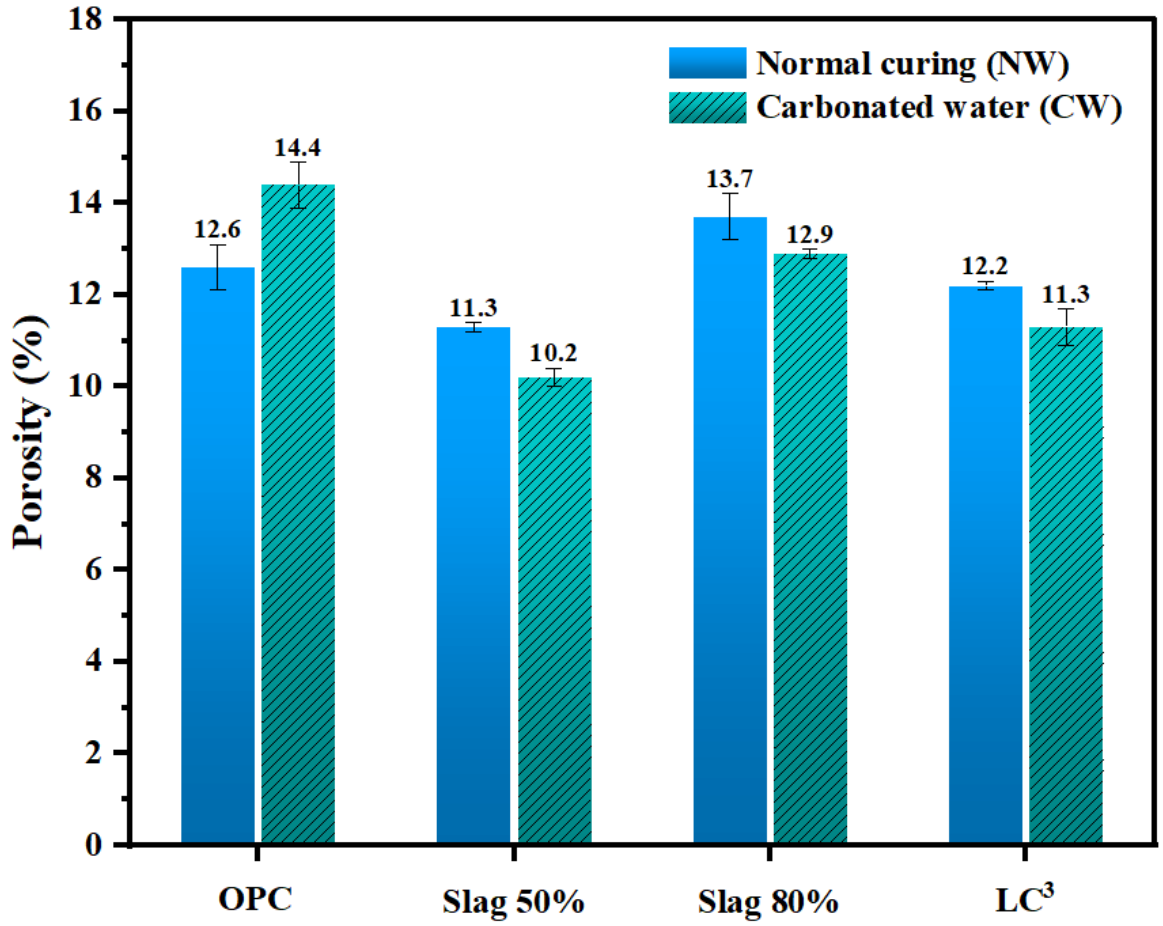


***Figure 11**: Porosity plot of the various cement systems with normal and carbonated water*

The increased sorptivity and porosity noted in OPC align with findings by Dos Santos et al., 2019, and Suescum-Morales et al., 2022, who reported a 5% increase in accessible porosity when carbonated water is used. In OPC systems, carbonated water induces the early formation of dense carbonate coatings which hinder further hydration. This surface passivation causes initial hydration retardation, limiting the formation of hydration products necessary for pore refinement. Consequently, the pores remain more connected, resulting in increased sorptivity and porosity. In studies where CO_2 was introduced in gaseous form during mixing (Monkman et al., 2016; Rashid and Singh, 2023), improvements or neutral trends in transport properties, such as chloride migration and sorptivity, were reported. It is noteworthy that the CO_2 dosages examined in those studies (0.05-0.2% by weight of cement) were substantially lower than those explored in the present work.

By contrast, as discussed earlier in the strength results, the improved durability observed in low-carbon cements arises from the formation of calcium carboaluminate phases, predominantly derived from interactions between C_3A and its hydration products with CO_2. These precipitates effectively fill pores in the matrix, densifying the microstructure and reducing pore connectivity, thereby lowering sorptivity and porosity (Xia et al., 2023). Additionally, carbonation accelerates C_3S hydration kinetics in these systems, promoting the formation of solid hydration products that further refine the pore structure.

Early-age carbonation has been reported in prior studies to reduce the percentage of permeable voids through the formation of solid calcite (Liu 2016; Liang et al., 2024). However, the collapse and restructuring of C-S-H can substantially diminish micropores. Furthermore, calcium carbonate precipitation may occlude gel pores, thereby shifting the pore size distribution toward larger diameters, increasing the critical pore diameter, and inducing coarsening of the overall pore structure (Gu et al., 2025). Consequently, the overall effect can be thought to be governed by the balance between calcite formation and C-S-H degradation in OPC and low-carbon cements, with their cumulative influences determining performance under various deterioration mechanisms. Thus, the beneficial pore-filling effects of carbonated water dominate in low-carbon cements due to their composition and the balanced interplay between carbonation and hydration, whereas in OPC, it leads to microstructural degradation and reduced durability.

6.3 Microstructural properties

6.3.1 TGA

The TGA plots for all paste types tested with normal and carbonated water are shown in Figures 12 to 15. In these plots, the TG Y-axis indicates mass loss, while the DM Y-axis shows the rate of mass change, corresponding to specific decomposition phases. These plots identify the

608 phases based on mass losses at various temperatures, as indicated in the figures. Notably, mass
609 losses associated with ettringite (AFt), C-S-H, monosulfoaluminate (AFm),
610 hemicarboaluminates (Hc) and monocarboaluminates (Hm) phases overlap within the 100-
611 300°C temperature range. Consequently, these phases are reported collectively for this range,
612 as precise determination of individual mass percentages is not feasible.

613 Distinct peaks corresponding to AFt and C-S-H are evident across all cement types. All cement
614 systems except for LC^3 exhibit definite portlandite peaks, with intensities decreasing as SCM
615 replacement increases relative to OPC. Interestingly, LC^3 is the only system showing distinct
616 AFm phases. This observation, in conjunction with calorimetry results indicating significant
617 enhancement of C_3A hydration activity in LC^3 carbonated water mixes, suggests that AFm and
618 AFt phases may serve as potential binding sites for carbonate ions. This interpretation is further
619 supported by the TGA curves of LC^3, which show a pronounced increase in mass rate curve in
620 the C-S-H/AFt phase, followed by a smaller but clear increase in the AFm phase. In slag-50%
621 systems, a moderate reduction in portlandite (0.5%) is observed alongside an increase in calcite
622 phases (1%), the latter resulting primarily from the carbonation of portlandite. Conversely,
623 OPC shows minimal peak changes except for a distinct peak around 800-900 ºC, attributed to
624 the wollastonite-like decomposition of C-S-H phases at elevated temperatures, as previously
625 documented by Myers et al., 2015 in their study of C-S-H hydrates. This thermal transformation
626 is absent in low-calcium cements, likely due to their reduced Ca/Si ratios (Richardson, 1999;
627 Richardson et al., 2002), which promote longer silicate chain-length hydrates with enhanced
628 thermal stability that resist conversion of C-S-H to wollastonite upon heating, as reported
629 earlier (Tajuelo Rodriguez et al., 2017). Collectively, TGA analysis demonstrates that only LC^3
630 systems exhibited profound phase changes upon CO_2 binding followed by slag systems,
631 indicating a stronger interaction and effect of carbonated water in these binders compared to
632 others.

Despite the pronounced phase changes observed in LC^3, overall mass loss percentages derived from the TGA plots reveal minimal differences between normal and carbonated water, with variations typically ranging from 2-4% for certain phases and even smaller variations for most other phases across all cement types. While TGA provides valuable phase identification insights for both normal and carbonated water systems, caution is warranted when interpreting specific effects of carbonation on individual hydration phases due to overlapping decomposition peaks. Therefore, XRD analysis was performed to further clarify phase transformations.

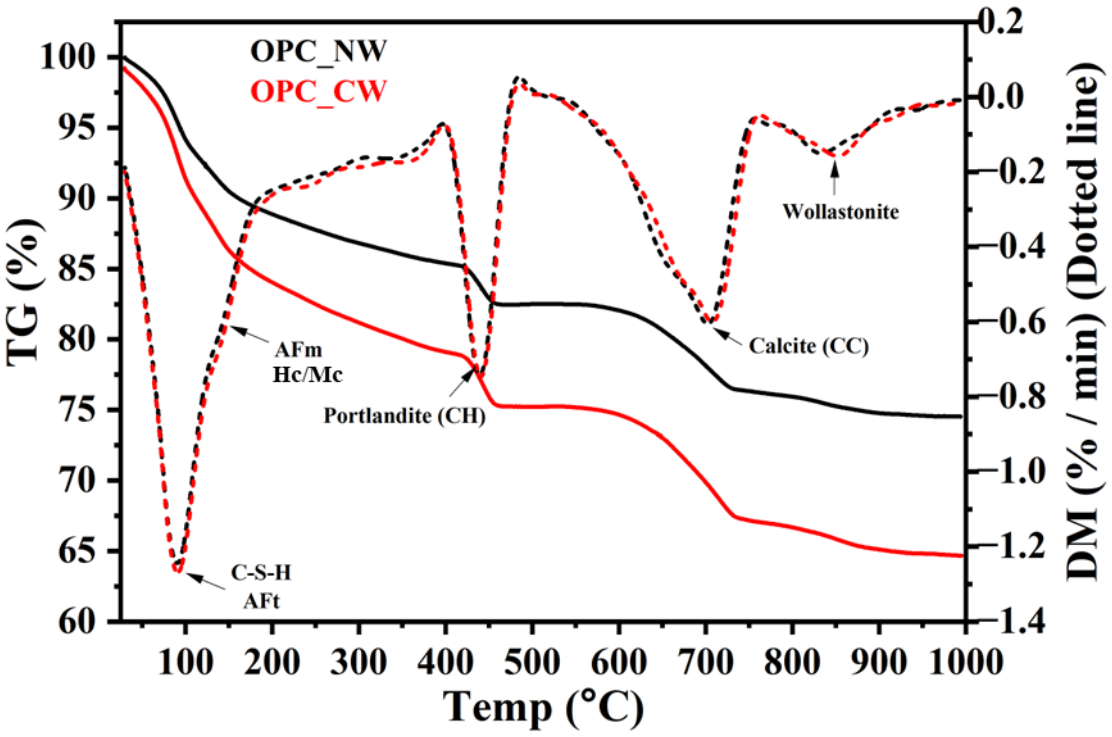
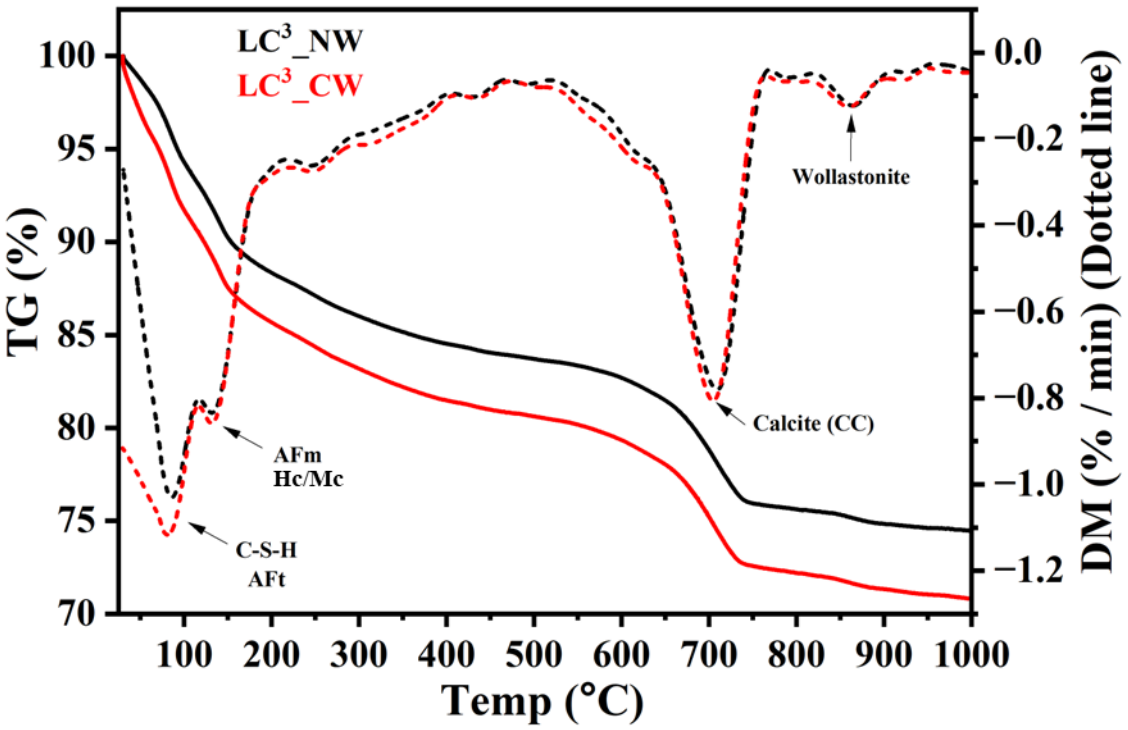
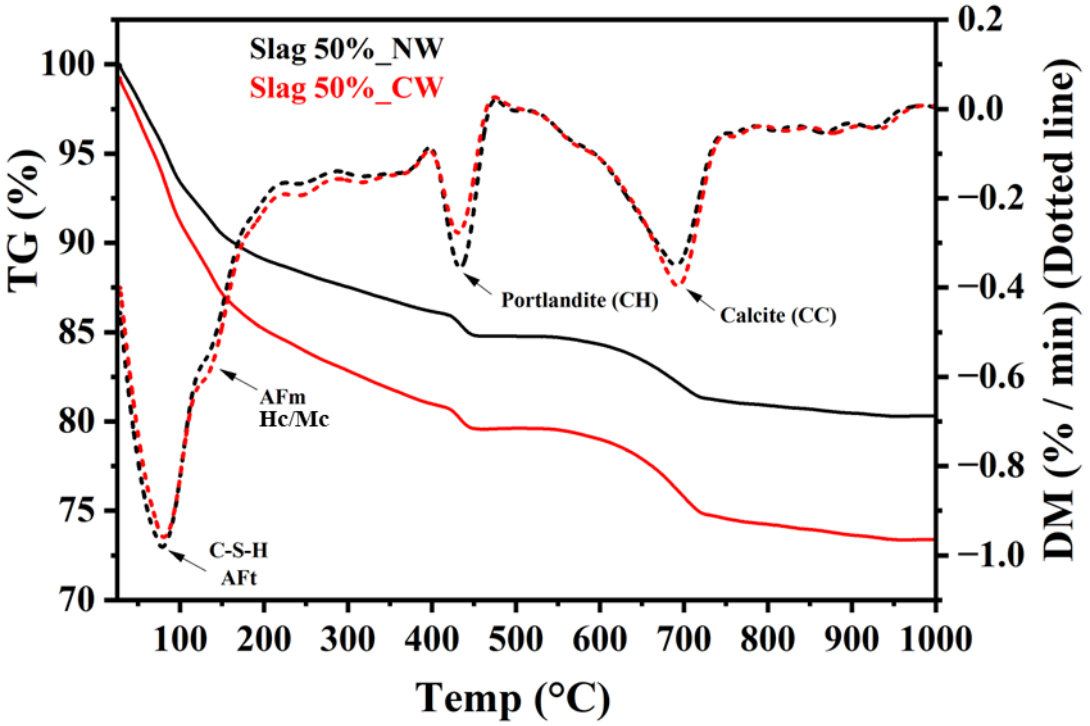


Figure 12: *TGA plots of OPC paste with normal and carbonate water*



643

644 ***Figure 13:*** *TGA plots of LC^3 paste with normal and carbonate water*



645

646 ***Figure 14:*** *TGA plots of Slag 50% paste with normal and carbonate water*

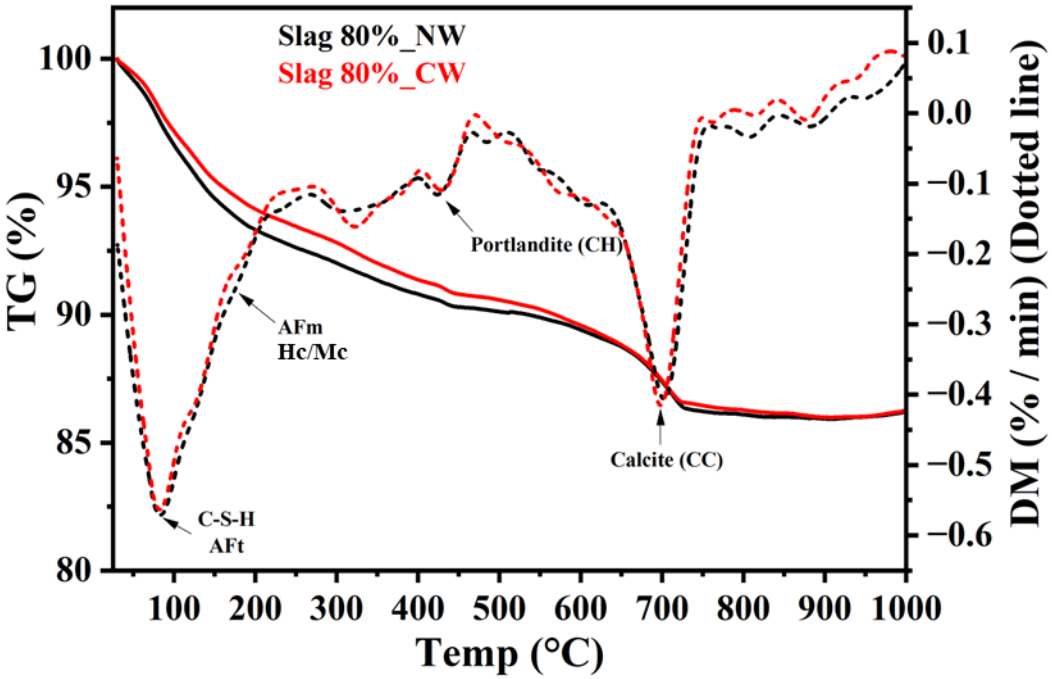


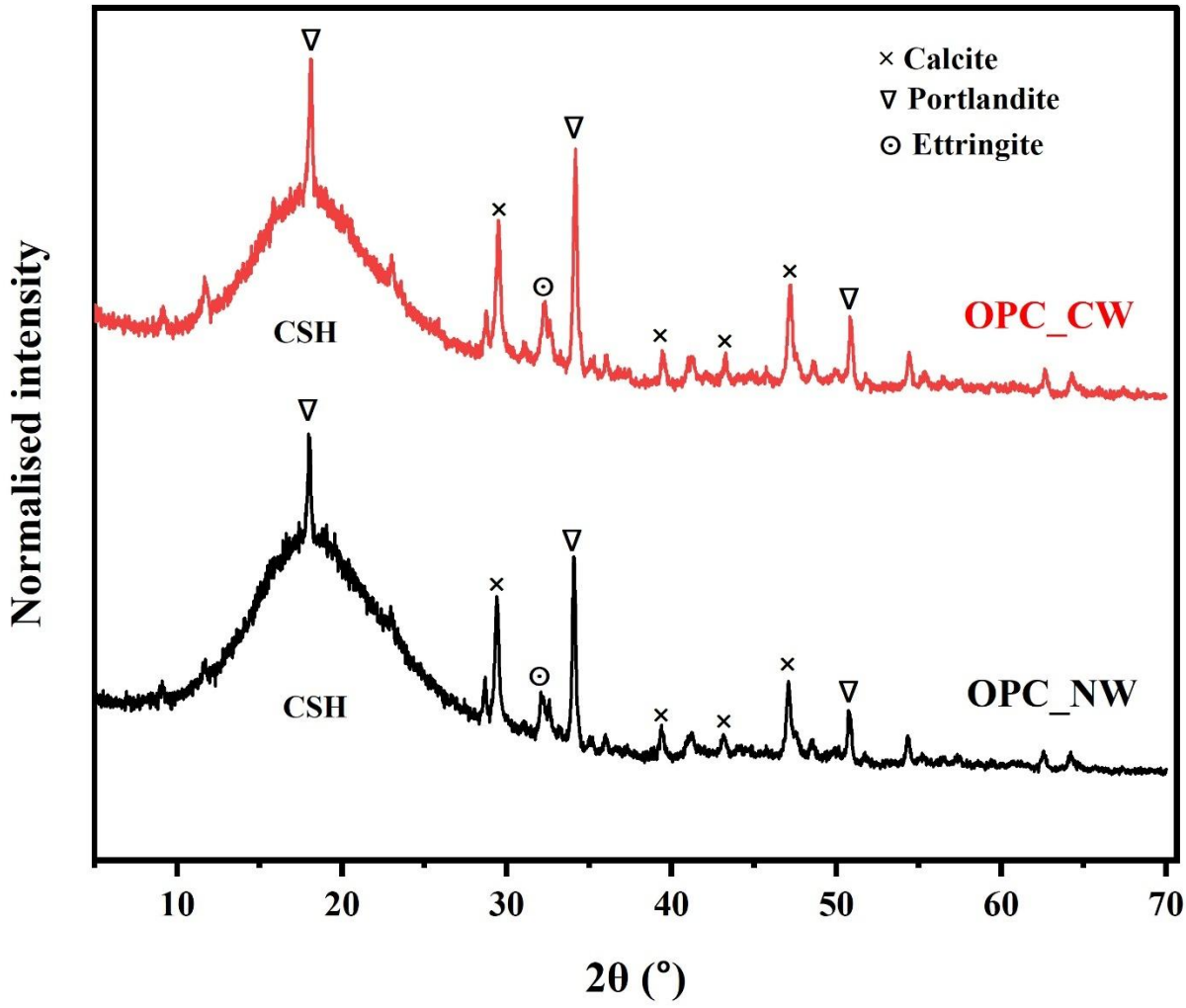
Figure 15: *TGA plots of Slag 80% paste with normal and carbonate water*

6.3.2 XRD

The XRD analysis of powdered paste samples with both normal and carbonated water reveals distinct carbonation behaviours across the different cement types investigated (Figures 16 to 19). The primary phases identified include the amorphous humps of C-S-H and its decalcified silica gel forms, alongside peaks corresponding to calcite, monocarboaluminates, and portlandite. Notably, the most pronounced effect observed in the XRD spectra is the carbonation of C-S-H, transforming it into decalcified amorphous silica gels. Semi-crystalline peaks of C-S-H, as observed in synthetic C-S-H samples in previous studies, typically appear around 16º and 29º, while the amorphous silica gel hump is centred around 18º (Liu et al., 2022). The transformation of C-S-H gel towards decalcified or lower Ca/Si ratio forms is distinctly noted in the slag-50% and slag-80% mixes by an amorphous hump centred around 18º, spanning from 15º to 28º, under the influence of carbonated water. Studies (Lu et al., 2023) using XRD on carbonation of C-S-H gels have attributed these amorphous humps to the formation of calcium-modified silica gels due to carbonation. The reduction in peak intensities

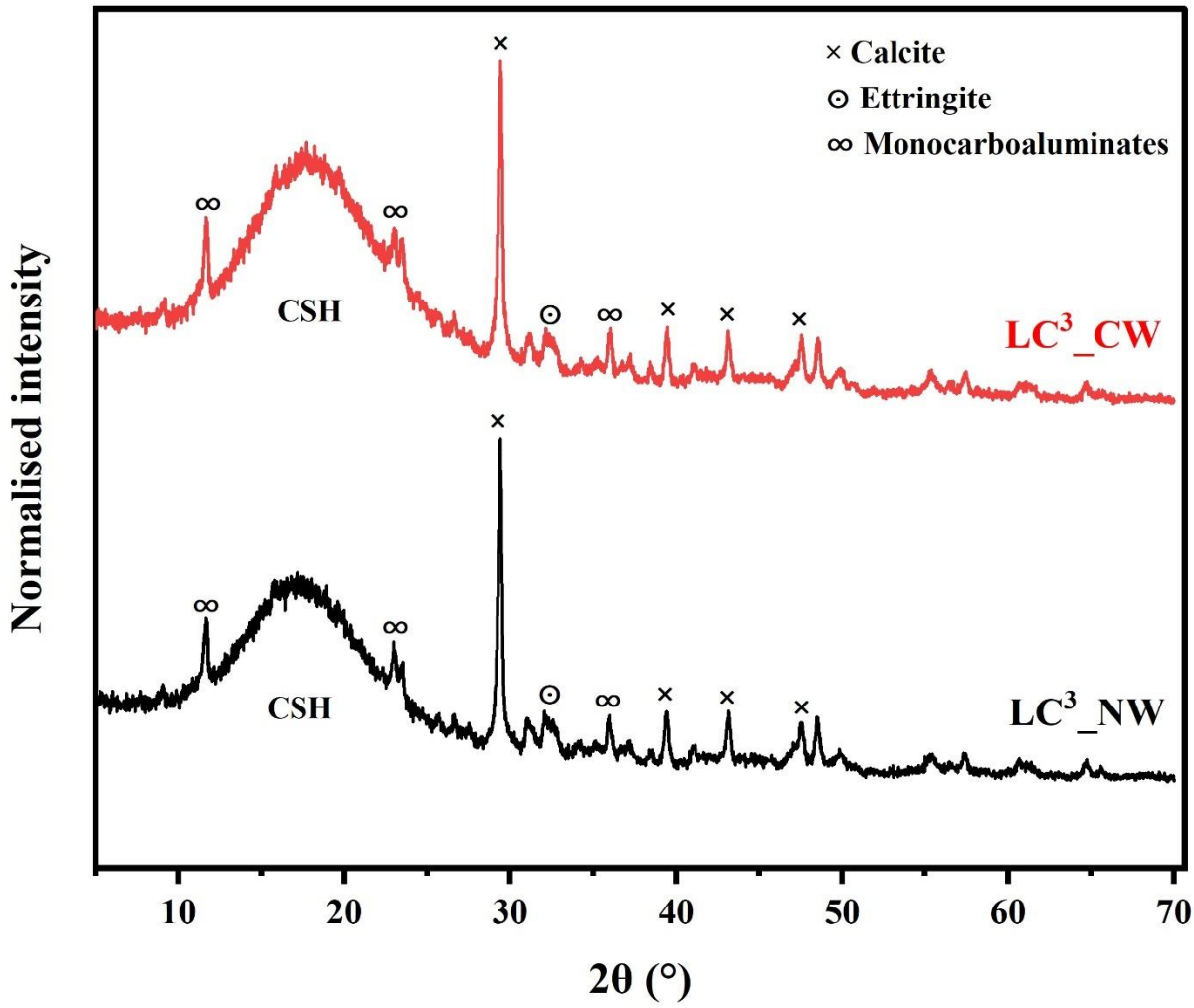
663 of C-S-H at 29º in the slag cement pastes further supports the decalcification of C-S-H under
664 carbonated water. Previous studies (Baston et al., 2012; Xin et al., 2017) have also reported
665 similar amorphous C-S-H peaks in carbonated slag mixes, linked to C-S-H with low Ca/Si
666 ratios (approximately 0.6), confirming carbonation of C-S-H in them. The formation of such
667 amorphous silica gels indicates calcium release from the silicate chains, resulting in gels with
668 lower molar volume and a coarser pore network relative to intact C-S-H. This transformation
669 increases overall porosity and permeability while diminishing the binding capacity of the gel,
670 as reported previously (Liu et al., 2023; Morandeau et al., 2014; Wu & Ye, 2017).

671 In contrast, OPC and LC^3 were characterised by amorphous humps from 15 to 29º under both
672 normal and carbonated water conditions. Hence, unlike slag systems, these amorphous humps
673 in OPC and LC^3 are attributed to C-S-H gels. While C-S-H typically shows diffracted peaks
674 around 16º, the larger volume of C-S-H formed in OPC and LC^3 systems likely caused a
675 broader spread in the XRD spectra. It is interesting to note that the C-S-H hump in OPC showed
676 reduced spread and intensity in carbonated water mix compared to normal water, indicating a
677 decrease in C-S-H content. However, this reduction was not observed in LC^3, suggesting a
678 more stable C-S-H structure in LC^3 under carbonated water. Also, the diffracted peaks of
679 C-S-H in OPC and LC^3 at 29º showed minimal changes in carbonated water mixes, with other
680 peaks for calcite and portlandite also exhibiting less pronounced changes in these systems.
681 Although Zajac et al., 2022 reported decalcified C-S-H XRD humps only in carbonated OPC
682 samples, akin to those in slag systems, the XRD spectra of OPC and LC^3 in this study did not
683 show similar pattern at the tested CO_2 dosage.



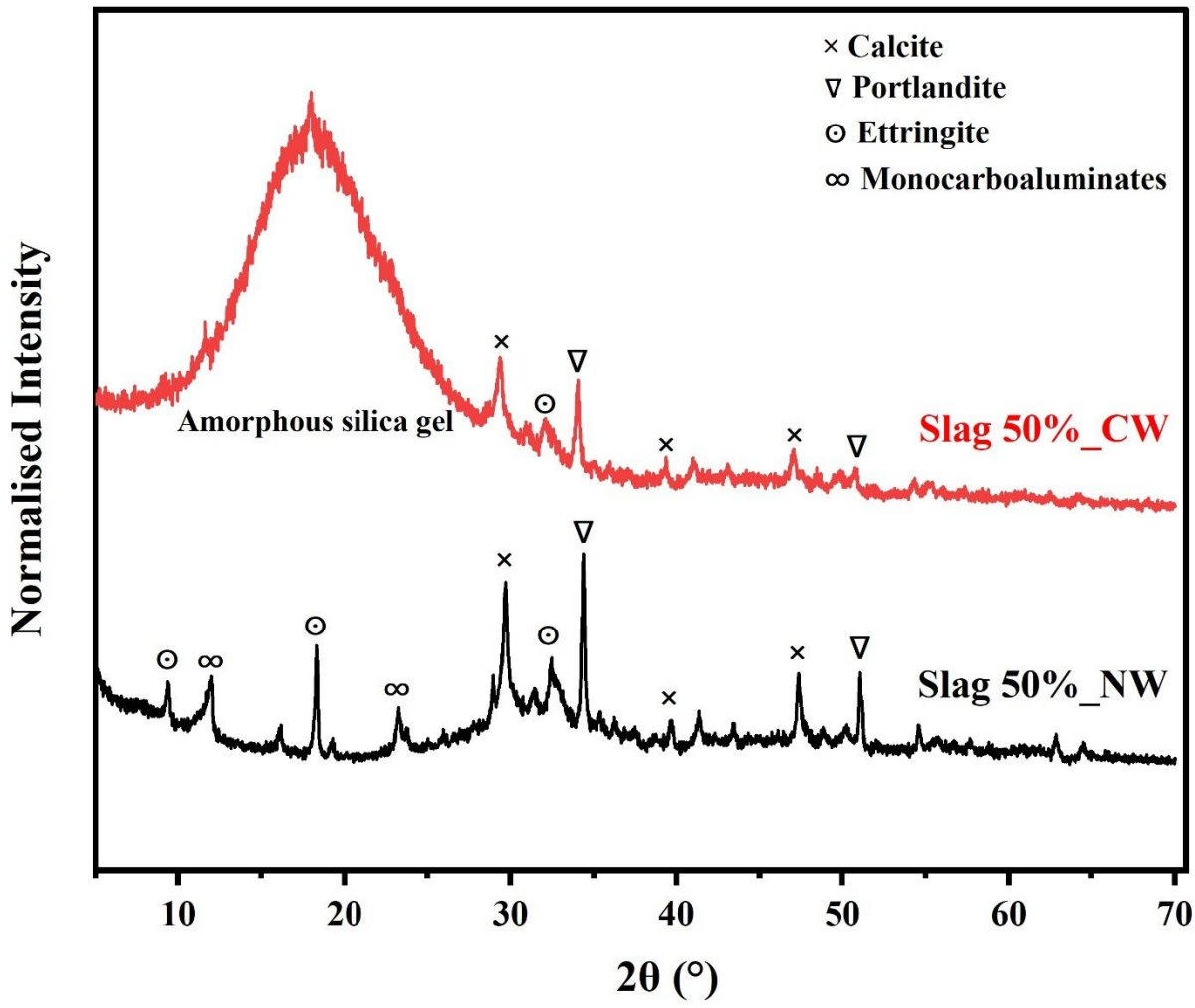
684

685 ***Figure 16:*** *XRD plots of OPC paste with normal and carbonate water*



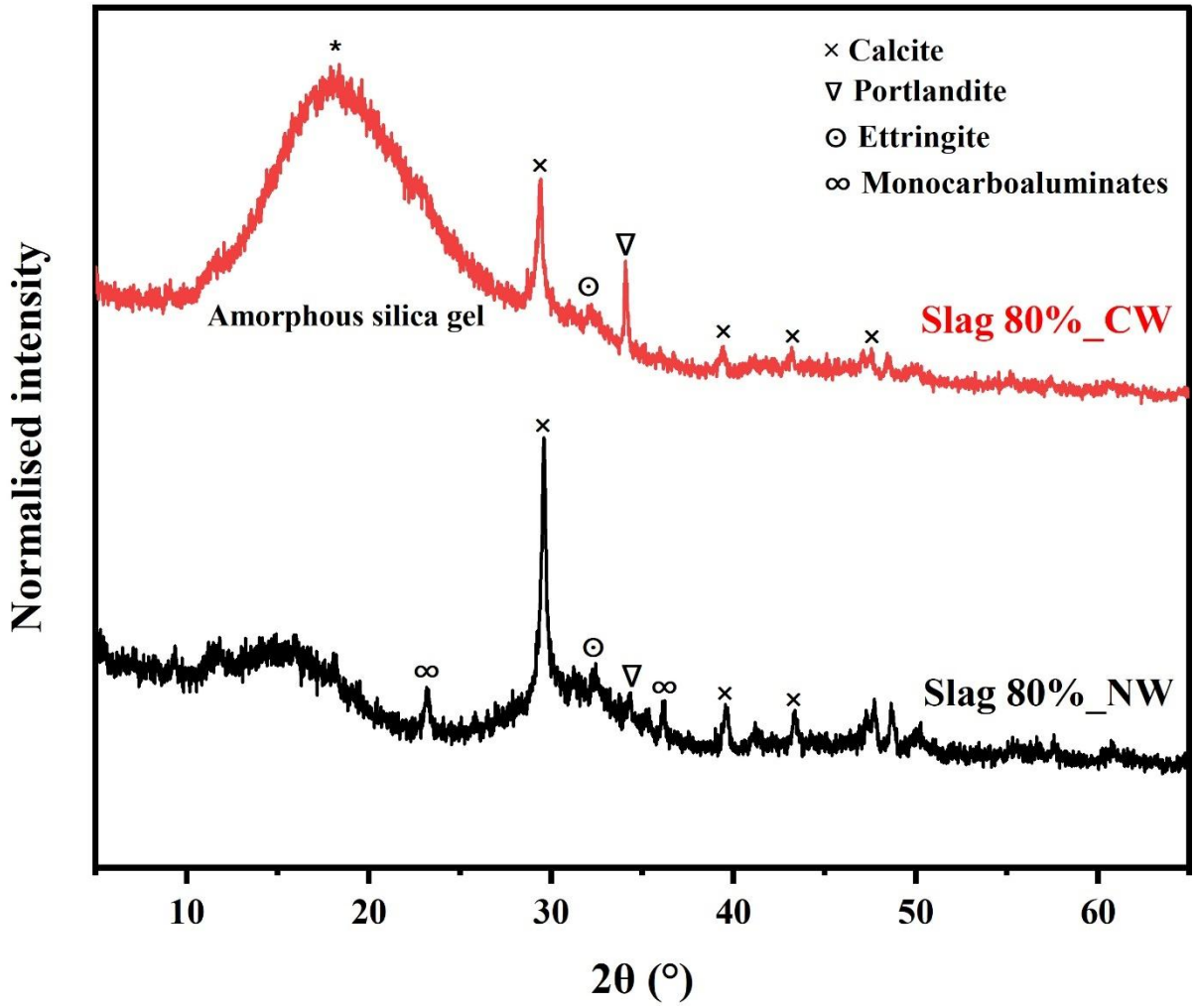
686

687 ***Figure 17:*** *XRD plots of LC^3 paste with normal and carbonate water*



688

689 ***Figure 18:*** *XRD plots of Slag 50% paste with normal and carbonate water*



690

691 ***Figure 19:*** *XRD plots of Slag 80% paste with normal and carbonate water*

692 Interestingly, while isothermal calorimetry indicated enhanced C_3A activity across all systems,
693 suggesting CO_2 binding in ettringite and monocarboaluminates, XRD revealed substantial C-
694 S-H gel alterations, particularly in slag systems, with minimal evidence of carbonated
695 ettringite. Rietveld quantification was not performed to determine the exact phase contents due
696 to the presence of pronounced amorphous humps from C-S-H and other poorly crystalline
697 carbonated phases, which obscured clear distinction between amorphous hydration products
698 and carbonation-derived phases such as amorphous calcite. This limitation highlights a
699 potential direction for a more detailed investigation in future studies.

700 Variations in XRD patterns for carbonated forms of the different cement systems can be
701 attributed to differences in their chemical composition, specifically the levels of calcium oxide

(CaO), aluminum oxide (Al_2O_3), and sulfur trioxide (SO_3), which influence the formation and stability of their hydrates (Damidot et al, 2007). For example, while LC^3 cement exhibited the highest C_3A activity from isothermal calorimetry, it was the slag cement types which showed the greatest amorphous transformation of C-S-H in their carbonated forms. This difference likely results from the distinct chemical makeup of the cements, leading to variations in the C-S-H structure and consequently, its CO_2 binding. Another notable observation is that slag cement types exhibited lower calcite formation in carbonated water mixes, while OPC and LC^3 systems showed either marginal increases or consistent calcite peak levels upon carbonation. A previous study by Kim et al., 2024 on OPC-based fresh-state carbonation reported that while calcite crystals were formed, they existed in poorly crystalline phases undetectable by XRD. This suggests that the lower calcite formation observed in slag cement systems may result from calcite existing in poorly crystalline phases or that calcite is not the primary carbonation product in these systems. This observation also supports the possibility of simultaneous CO_2 binding in C-S-H and portlandite in low-carbon cements with low Ca/Si ratios, suggesting that decalcified silica gel formation may occur concurrently with, rather than solely following, portlandite carbonation as generally reported ((Von Greve-Dierfeld et al., 2020). It could also mean that the pozzolanic reaction in slag-high systems consumed portlandite, reducing the free calcium available to react with carbonate ions, which also lead to lower amounts of calcite formation. Thus, CO_2 binding in slag cements seems to primarily influence C-S-H transformations, indicating distinct carbon binding pathways compared to OPC and LC^3 cements.

7. CO_2 BINDING DRIVERS IN CEMENT SYSTEMS: BEYOND THE CALCIUM CONTENT

While calcium content remains the fundamental basis for theoretical models estimating CO_2 sequestration capacity in cements, it is equally important to understand the factors that govern

727 calcium dissolution or its inhibition. This is particularly significant since the introduction of
728 CO_2 can alter solution kinetics, thereby affecting calcium dissolution and ultimately the actual
729 extent of CO_2 binding.

730 With this perspective, pH and the corresponding H^+ ion concentration emerges as the most
731 critical drivers of aqueous carbonation, exerting a twofold effect. At high pH, CO_2 exhibits
732 increased solubility, facilitating its incorporation into the system, whereas lower pH promotes
733 the dissolution of calcium from cement phases, enhancing CO_2 binding through $CaCO_3$
734 formation. Thus, while high pH supports CO_2 dissolution, lower pH accelerates the reaction
735 between CO_2 and calcium, contributing to effective carbonation (Goetz-Neunhoeffer et al.,
736 2006). Cement systems with higher initial pH levels such as OPC showed a more pronounced
737 decrease in H^+ ion concentration upon exposure to carbonated water. This suppresses calcium
738 dissolution and reduces hydration of C_3S phases, which is an unfavourable outcome of carbon
739 sequestration. Conversely, low-carbon cements, with their lower initial pH and free hydroxide
740 ions, have a reduced ability to neutralise carbonic acid. This leads to greater CO_2 availability
741 for binding and enhanced calcium dissolution, promoting increased hydration in these cement
742 systems.

743 This nuanced role of pH and ion concentration aligns with previous findings on gaseous CO_2
744 injection on OPC (Kim et al., 2024), which suggested that combining air mixing with CO_2
745 injection could mitigate pH effects on CO_2 uptake. Building on these insights, a pragmatic
746 phased approach of initially employing normal water mixing to maintain stable pH conditions,
747 followed by the controlled incremental addition of carbonated water could help mitigate
748 adverse pH fluctuations and optimise CO_2 binding. This approach, however, requires practical
749 verification at the pilot scale.

Additionally, calcium ions in solution further modulate CO_2 binding behaviour. While calcium ion presence can inhibit C_3S dissolution (Suraneni, 2015), carbonate ions sequester calcium, reducing free Ca^{2+} concentration and promoting faster hydration, as seen in low-carbon cements. In contrast, slower C_3A hydration increase in OPC under carbonated water limits CO_2 binding with hydration products, leaving more free Ca^{2+} ions available. Together with pH effects, this may retard further C_3S hydration in OPC. Thus, contrary to expectations that calcium-rich cements would bind CO_2 more effectively, high-calcium OPC may experience greater hydration delays that limit the effectiveness of carbonated water for sequestration.

In addition to pH and C_3S dissolution, this study highlights the significant role of C_3A in CO_2 sequestration. The enhanced hydration of C_3A in the presence of carbonated water suggests that CO_2 may become incorporated within its hydration products, such as ettringite or monosulfate, depending on the gypsum content. However, ettringite can convert to monosulfoaluminate, a more stable but less CO_2 reactive phase (Christensen et al., 2004). Previous studies, such as those by Kuzel & Pollmann (Kuzel and Pöllmann, 1991), have shown that the presence of carbonate ions inhibits this conversion. This inhibition is advantageous for carbon sequestration, as it promotes the retention of more reactive ettringite and thus enhances CO_2 binding. XRD analysis, however, revealed that not all forms of ettringite exhibit enhanced CO_2 binding. Slag-based cement systems displayed the highest levels of amorphous carbonated C-S-H, whereas carbonated OPC systems showed only a marginal increase in calcite formation compared to their normal water mixes. These findings underscore the complexity of factors influencing CO_2 binding, and despite significant C_3A hydration under carbonated water, the lack of evidence of carbonated ettringite observed in this study, warrants further investigation.

8. CONCLUSIONS AND RECOMMENDATIONS

This study critically re-evaluates the common hypothesis that effective CO_2 sequestration in cement is governed solely by bulk calcium content, asserting instead that it depends on maintaining favourable calcium dissolution kinetics through the precise interplay between early hydration products, pH, and calcium chemistry. Among the cement types tested, low-carbon formulations, specifically LC^3 and Slag-50%, optimally balance this chemistry, resulting in superior CO_2 binding with carbonated water compared to high-calcium OPC systems.

Crucially, the use of carbonated water in these low-carbon cements offers dual benefits: it accelerates delayed setting times (particularly in slag-80% blends) and modifies hydration kinetics, notably increasing C_3A hydration in LC^3 and slag-80% systems. This synergistic effect leads to notable compressive strength gains and improved durability, evidenced by reduced sorptivity and porosity in the low-carbon cements tested. Conversely, conventional OPC experiences modest strength losses and increased sorptivity with CO_2 binding, underscoring that CO_2 sequestration is not a universal sustainability opportunity but a potential durability risk for certain cement systems. Therefore, parallel to efforts advancing the technical potential of cement-based CO_2 sequestration, it is imperative that research is directed toward identifying cementitious systems that reconcile sustainability goals with long-term durability under CO_2 binding. It should be noted, however, that the performance reported herein is specific to the dosage employed, and the observed trends may vary at higher dosages, where a greater proportion of the intrinsic hydration phases could be influenced by CO_2 binding. Furthermore, the potential effects of using carbonated water on other deterioration mechanisms should be investigated to better inform its practical implementation and facilitate broader adoption.

The extent of direct CO_2 sequestration achieved through the use of carbonated water under the investigated conditions remains relatively limited on a volumetric basis, estimated at approximately 1-2 kg/m^3. However, this estimate does not include the secondary benefits associated with strength enhancement and durability improvements, which may contribute to additional indirect carbon savings through reduced cement consumption over the service life of the material. Achieving aggressive net-zero targets will require broader mineralisation strategies, focusing on locking CO_2 in inert phases such as aggregates used in large volumes, and in waste materials that offer avoided emissions reduction co-benefits, to achieve more substantial sequestration outcomes.

818 **SUPPLEMENTARY DATA**



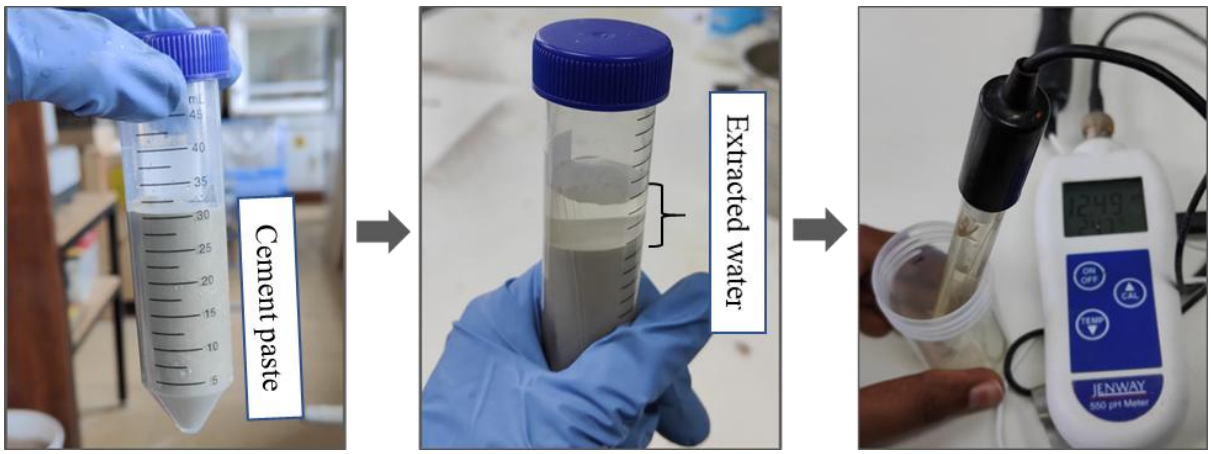
819

820 **Figure S1:** (a) Casting of mortar specimens, and (b) sealed water curing set-up



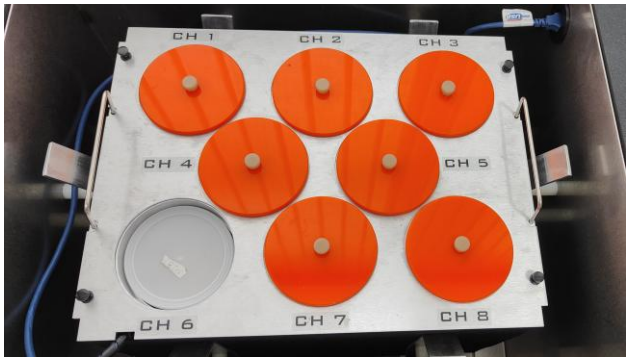
821

822 **Figure S2:** Flow of mortars in flow table test



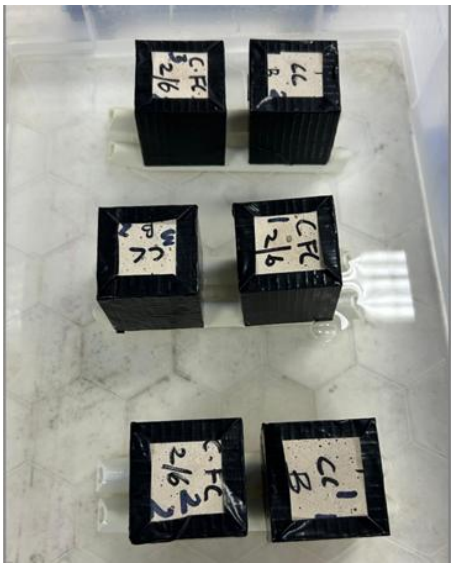
823

824 **Figure S3:** Test procedure for measuring the pH of paste samples



825

826 **Figure S4:** Specimens mounted in the isothermal calorimeter



827

828 **Figure S5:** Sorptivity test setup with one specimen face exposed to water for capillary water
829 absorption measurement

830

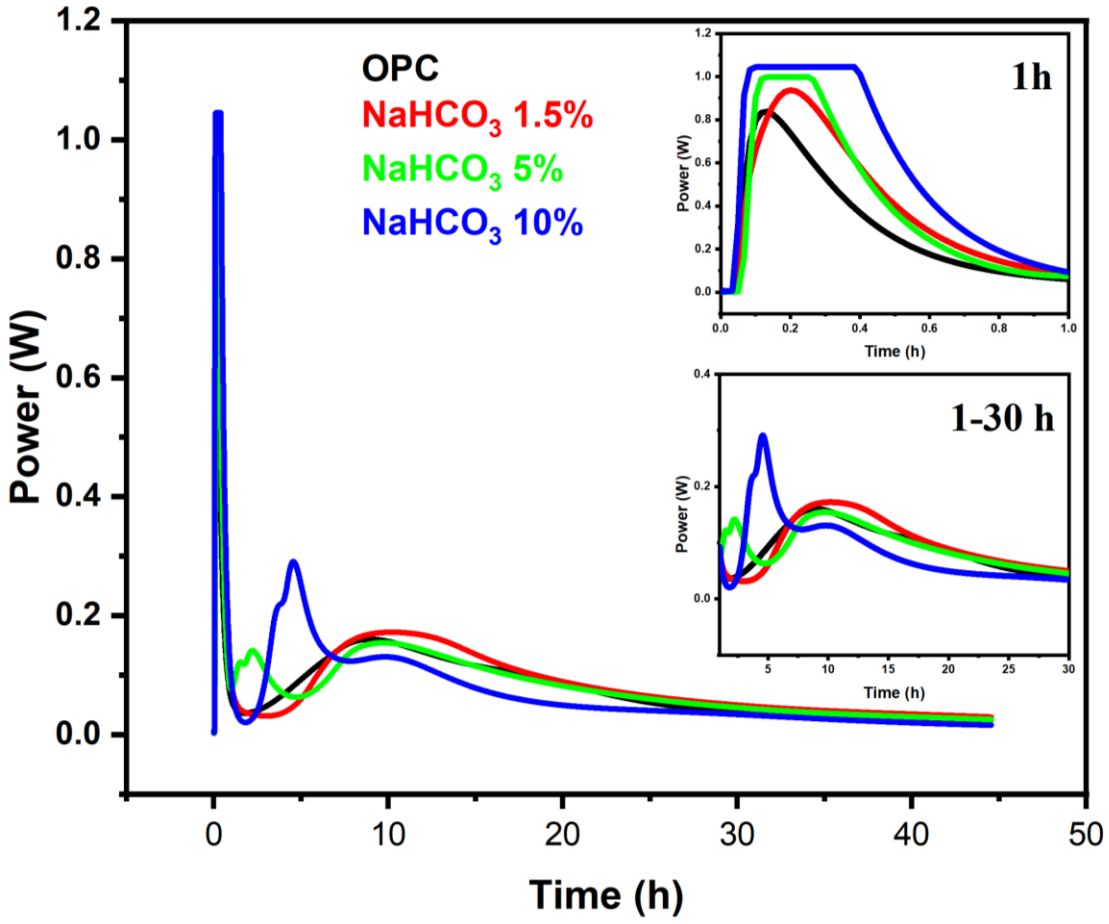


Figure S6: Isothermal Calorimetry Plot comparing various dosages of $NaHCO_3$ with OPC paste samples

ACKNOWLEDGEMENTS

The first author gratefully acknowledges the UK Engineering and Physical Sciences Research Council (EPSRC) for funding this research through the EPSRC Centre for Doctoral Training in Future Infrastructure and Built Environment: Resilience in a Changing World (FIBE2 CDT) (EPSRC grant reference number EP/S02302X/1).

CRedit AUTHORSHIP CONTRIBUTION STATEMENT

Aswathy Rajendran: Writing – original draft, Visualization, Methodology, Investigation, Validation, Data curation, Formal analysis. **Sripriya Rengaraju:** Writing – review and editing,

Methodology, Validation, Supervision. **Abir Al-Tabbaa:** Writing – review and editing, Funding acquisition, Supervision.

DECLARATION OF GENERATIVE AI AND AI-ASSISTED TECHNOLOGIES IN THE WRITING PROCESS

During the preparation of this work, the first author used Grammarly and ChatGPT to review grammar and proofread certain sections of the article. After utilising these tools, the author reviewed and edited the content as needed and takes full responsibility for the final content of the publication.

REFERENCES

Aghaee, K., 2025. Carbon capture, utilization, and storage for sustainable construction: Insights into CO_2 mixing, curing, and mineralization. Carbon Capture Sci. Technol. 17, 100503. https://doi.org/10.1016/j.ccst.2025.100503

ATM C191, Standard test methods for time of setting of hydraulic cement by Vicat needle, ASTM international, 2021

ASTM C1585, Standard test method for measurement of Rate of Absorption of Water by Hydraulic-cement concretes, ASTM International, 2020

Baston, G.M.N., Clacher, A.P., Heath, T.G., Hunter, F.M.I., Smith, V., Swanton, S.W., 2012. Calcium silicate hydrate gel dissolution and pH buffering in a cementitious near field. Mineral. Mag. 76, 3045–3053. https://doi.org/10.1180/minmag.2012.076.8.20

Bhandari, I., Kumar, R., Sofi, A., Nighot, N.S., 2023. A systematic study on sustainable low carbon cement-Superplasticizer interaction: Fresh, mechanical, microstructural and durability characteristics. https://doi.org/10.1016/j.heliyon.2023.e19176

Biava, G., Depero, L.E., Bontempi, E., 2024. Accelerated Carbonation of Steel Slag and Their Valorisation in Cement Products: A Review. Span. J. Soil Sci. 14, 12908. https://doi.org/10.3389/sjss.2024.12908

BS EN 1015-11, Methods of test for mortar for masonry: Determination of flexural and compressive strength of hardened mortar, British standard Institution, https://doi.org/10.3403/BSEN1015

BS EN 13139, Aggregates for mortar, British standard Institution, 2013

Ramachandran, V.S & Chun-Mei, Z., 1986. Hydration kinetics and microstructural development in the $3CaO.Al_2O_3$-$CaSO_4.2H_2O$-$CaCO_3$-H_2O system. Mater. Struct. 19, 437-444. https://doi.org/10.1007/BF0247

Cao, M., Ming, X., He, K., Li, L., Shen, S., 2019. Effect of Macro-, Micro- and Nano-Calcium Carbonate on Properties of Cementitious Composites—A Review. Materials 12, 781. https://doi.org/10.3390/ma12050781

Carlson, E.T., Berman, H.A., 1960. Some observations on the calcium aluminate carbonate hydrates. J. Res. Natl. Bur. Stand. Sect. Phys. Chem. 64A, 333. https://doi.org/10.6028/jres.064A.032

Celia, M.A., 2017. Geological storage of captured carbon dioxide as a large-scale carbon mitigation option. Water Resour. Res. 53, 3527–3533. https://doi.org/10.1002/2017WR020841

Chang, Y., Gao, S., Ma, Q., Wei, Y., Li, G., 2024. Techno-economic analysis of carbon capture and utilization technologies and implications for China. Renew. Sustain. Energy Rev. 199, 114550. https://doi.org/10.1016/j.rser.2024.114550

Chen, J., Xie, B., Lu, Z., He, S., Ma, S., 2025. Early Hydration Characteristics and Kinetics Model of Ordinary Portland Cement-Calcium Sulfoaluminate Cement Composites. Materials 18, 2559. https://doi.org/10.3390/ma18112559

Christensen, A.N., Jensen, T.R., Hanson, J.C., 2004. Formation of ettringite, $Ca_6Al_2(SO_4)_3(OH)_{12}\cdot 26H_2O$, AFt, and monosulfate, $Ca_4Al_2O_6(SO_4)\cdot 14H_2O$, AFm-14, in hydrothermal hydration of Portland cement and of calcium aluminum oxide—calcium sulfate dihydrate mixtures studied by in situ synchrotron X-ray powder diffraction. J. Solid State Chem. 177, 1944–1951. https://doi.org/10.1016/j.jssc.2003.12.030

Stripple, H., Ljungkrantz, C., Gustafsson, T., Andersson, R., 2018. CO_2 uptake in cement-containing products. Background and calculation models for IPCC implementation. IVL Swedish Environmental Research Institute, Report B 2309, ISBN: 978-91-88787-89-7

Damidot, D., Bellmann, F., Moser, B., Sovoidnich, T., 2007. Investigation of the early dissolution behavior of C_3S. Conference proceedings: 12th international congress on the chemistry of cement, Montreal, Canada

Davolio, M., Muciaccia, G., Ferrara, L., 2025. Concrete carbon mixing – A systematic review on the processes and their effects on the material performance. Clean. Mater. 15, 100292. https://doi.org/10.1016/j.clema.2025.100292

De Weerdt, K., Plusquellec, G., Belda Revert, A., Geiker, M.R., Lothenbach, B., 2019. Effect of carbonation on the pore solution of mortar. Cem. Concr. Res. 118, 38–56. https://doi.org/10.1016/j.cemconres.2019.02.004

Dos Santos, V., Tonoli, G.H.D., Mármol, G., Savastano, H., 2019. Fiber-cement composites hydrated with carbonated water: Effect on physical-mechanical properties. Cem. Concr. Res. 124, 105812. https://doi.org/10.1016/j.cemconres.2019.105812

CEMBUREAU: 2050 Carbon neutrality roadmap 2020. The European Cement Association

Ferrari, L., Nagmutdinova, A., Müller, A., Mikanovic, N., Ben-Haha, M., Bortolotti, V., Franzoni, E., 2024. Water Retention in Calcined Clay: A Key Factor in the Rheological Challenges of Cement Mixtures. https://doi.org/10.2139/ssrn.5035709

Forsdyke, J., Lees, J., 2022. Carbonation behaviour of concrete exposed to natural and accelerated carbonation conditions. https://doi.org/10.17863/CAM.85412

Galan, I., Andrade, C., Mora, P., Sanjuan, M.A., 2010. Sequestration of CO_2 by Concrete Carbonation. Environ. Sci. Technol. 44, 3181–3186. https://doi.org/10.1021/es903581d

Gao, Z., Zhao, Q., Tao, M., Wang, Z., Liu, C., Saxén, H., Zevenhoven, R., 2024. Recent research progress on the direct carbon capture of steel slag to prepare building materials. Green Smart Min. Eng. 1, 387–395. https://doi.org/10.1016/j.gsme.2024.11.003

García Calvo, J., Sánchez Moreno, M., Alonso Alonso, M., Hidalgo López, A., García Olmo, J., 2013. Study of the Microstructure Evolution of Low-pH Cements Based on Ordinary Portland Cement (OPC) by Mid- and Near-Infrared Spectroscopy, and Their Influence on Corrosion of Steel Reinforcement. Materials 6, 2508–2521. https://doi.org/10.3390/ma6062508

Ghantous, R.M., Poyet, S., L'Hostis, V., Tran, N.-C., François, R., 2017. Effect of crack openings on carbonation-induced corrosion. Cem. Concr. Res. 95, 257–269. https://doi.org/10.1016/j.cemconres.2017.02.014

Goetz-Neunhoeffer, F., Neubauer, J., Schwesig, P., 2006. Mineralogical characteristics of Ettringites synthesized from solutions and suspensions. Cem. Concr. Res. 36, 65–70. https://doi.org/10.1016/j.cemconres.2004.04.037

Gu, H., Yang, Z., Sun, Y., Tao, Y., Zhang, Y., Jiang, W., 2025. Determination of pore structure evolution of cement paste under early-age carbonation by N2 isotherms. Constr. Build. Mater. 493, 143226. https://doi.org/10.1016/j.conbuildmat.2025.143226

Gunning, P.J., Hills, C.D., Carey, P.J., 2010. Accelerated carbonation treatment of industrial wastes. Waste Manag. 30, 1081–1090. https://doi.org/10.1016/j.wasman.2010.01.005

Han, S., Kim, J.H., Singh, R.K., Shah, S.P., 2025. CO2 utilization for cementitious materials - A review. KSCE J. Civ. Eng. 29, 100227. https://doi.org/10.1016/j.kscej.2025.100227

Hanifa, M., Agarwal, R., Sharma, U., Thapliyal, P.C., Singh, L.P., 2023. A review on CO2 capture and sequestration in the construction industry: Emerging approaches and commercialised technologies. J. CO2 Util. 67, 102292. https://doi.org/10.1016/j.jcou.2022.102292

Holmes, N., Russell, M., Davis, G., Tyrer, M., 2022. Comparing the Measured and Thermodynamically Predicted AFm Phases in a Hydrating Cement. Appl. Sci. 12, 10147. https://doi.org/10.3390/app121910147

Humagain, S., Shrestha, G., Madhavan, M.K., Sarker, P.K., 2025. Hydration, Soundness, and Strength of Low Carbon LC3 Mortar Using Waste Brick Powder as a Source of Calcined Clay. Materials 18, 3697. https://doi.org/10.3390/ma18153697

IS 18189, Portland calcined clay limestone cement, Bureau of Indian Standards, 2023.

Jakob, C., Jansen, D., Ukrainczyk, N., Koenders, E., Pott, U., Stephan, D., Neubauer, J., 2019. Relating Ettringite Formation and Rheological Changes during the Initial Cement Hydration: A Comparative Study Applying XRD Analysis, Rheological Measurements and Modeling. Materials 12, 2957. https://doi.org/10.3390/ma12182957

Juilland, P., Gallucci, E., Flatt, R., Scrivener, K., 2010. Dissolution theory applied to the induction period in alite hydration. Cem. Concr. Res. 40, 831–844. https://doi.org/10.1016/j.cemconres.2010.01.012

Kashef-Haghighi, S., Ghoshal, S., 2010. CO_2 Sequestration in Concrete through Accelerated Carbonation Curing in a Flow-through Reactor. Ind. Eng. Chem. Res. 49, 1143–1149. https://doi.org/10.1021/ie900703d

Kashef-Haghighi, S., Shao, Y., Ghoshal, S., 2015. Mathematical modeling of CO_2 uptake by concrete during accelerated carbonation curing. Cem. Concr. Res. 67, 1–10. https://doi.org/10.1016/j.cemconres.2014.07.020

Kazemian, M., Shafei, B., 2023. Carbon sequestration and storage in concrete: A state-of-the-art review of compositions, methods, and developments. J. CO2 Util. 70, 102443. https://doi.org/10.1016/j.jcou.2023.102443

Kim, J., Kim, D., Yun, T.S., 2023. Containment of sulfate in leachate as gypsum (CaSO4·2H2O) mineral formation in bio-cemented sand via enzyme-induced carbonate precipitation. Sci. Rep. 13, 10938. https://doi.org/10.1038/s41598-023-37772-z

Kim, N., Park, J., Amr, I.T., Bae, J.-H., Fadhel, B.A., Cho, A., Tay, S.Y., Seo, J., Lee, H.K., 2023. Hydration kinetics of ordinary Portland cement mixed under a direct CO_2 inject condition. J. Build. Eng. 77, 107531. https://doi.org/10.1016/j.jobe.2023.107531

Kim, W.K., Lee, J., Park, J., Moon, J., 2024. Carbon sequestration in cementitious systems through CO2-rich hydration and chemically enforced CO2 mineralization. J. CO_2 Util. 84, 102834. https://doi.org/10.1016/j.jcou.2024.102834

Kolani, B., Buffo-Lacarrière, L., Sellier, A., Escadeillas, G., Boutillon, L., Linger, L., 2012. Hydration of slag-blended cements. Cem. Concr. Compos. 34, 1009–1018. https://doi.org/10.1016/j.cemconcomp.2012.05.007

Kuzel, H.-J., Pöllmann, H., 1991. Hydration of C3A in the presence of $Ca(OH)_2$, $CaSO_4 \cdot 2H_2O$ and $CaCO_3$. Cem. Concr. Res. 21, 885–895. https://doi.org/10.1016/0008-8846(91)90183-I

Kwasny, J., Basheer, P.A.M., Russell, M., 2014. CO_2 Sequestration in Cement-Based Materials During Mixing Process Using Carbonated Water and Gaseous CO_2, in: Proceedings of the 4th International Conference on the Durability of Concrete Structures. Presented at the International Conference on the Durability of Concrete Structures, Purdue University Libraries Scholarly Publishing Services, pp. 72–79. https://doi.org/10.5703/1288284315385

Li, L., Hao, L., Li, X., Xiao, J., Zhang, S., Poon, C.S., 2023. Development of CO_2-integrated 3D printing concrete. Constr. Build. Mater. 409, 134233. https://doi.org/10.1016/j.conbuildmat.2023.134233

Li, Z., Bai, Y., Luo, Q., 2025. Influence of humidity conditions on the performance of CO_2-cured LC^3. Case Stud. Constr. Mater. 22, e04747. https://doi.org/10.1016/j.cscm.2025.e04747

Liang, C., Li, B., Guo, M.-Z., Hou, S., Wang, S., Gao, Y., Wang, X., 2024. Effects of early-age carbonation curing on the properties of cement-based materials: A review. J. Build. Eng. 84, 108495. https://doi.org/10.1016/j.jobe.2024.108495

Liu, L., Ji, Y., Gao, F., Zhang, L., Zhang, Z., Liu, X., 2021. Study on high-efficiency CO_2 absorption by fresh cement paste. Constr. Build. Mater. 270, 121364. https://doi.org/10.1016/j.conbuildmat.2020.121364

Liu, X., Feng, P., Cai, Y., Yu, X., Yu, C., Ran, Q., 2022. Carbonation behavior of calcium silicate hydrate (C-S-H): Its potential for CO_2 capture. Chem. Eng. J. 431, 134243. https://doi.org/10.1016/j.cej.2021.134243

Liu, Z., Van Den Heede, P., Zhang, C., Shi, X., Wang, L., Li, J., Yao, Y., Lothenbach, B., De Belie, N., 2023. Carbonation of blast furnace slag concrete at different CO2 concentrations: Carbonation rate, phase assemblage, microstructure and thermodynamic modelling. Cem. Concr. Res. 169, 107161. https://doi.org/10.1016/j.cemconres.2023.107161

Lu, B., Huo, Z., Xu, Q., Hou, G., Wang, X., Liu, J., Hu, X., 2023. Characteristics of CSH under carbonation and its effects on the hydration and microstructure of cement paste. Constr. Build. Mater. 364, 129952. https://doi.org/10.1016/j.conbuildmat.2022.129952

Suraneni, P., 2015. Micro-reactors to study hydration of cementitious materials. PhD Thesis. ETH Zurich

Moffatt, E. (Ted) G., Thomas, M.D.A., 2019. Effect of Carbonation on the Durability and Mechanical Performance of Ettringite-Based Binders. ACI Mater. J. 116. https://doi.org/10.14359/51710965

Moghul, S., Zunino, F., Flatt, R.J., 2025. Flow loss in superplasticized limestone calcined clay cement. J. Am. Ceram. Soc. 108, e20344. https://doi.org/10.1111/jace.20344

Monkman, S., MacDonald, M., Hooton, R.D., Sandberg, P., 2016. Properties and durability of concrete produced using CO2 as an accelerating admixture. Cem. Concr. Compos. 74, 218–224. https://doi.org/10.1016/j.cemconcomp.2016.10.007

Bonavetti, V.L., Rahhal, V.F., Irassar, E.F., 2001. Studies on the carboaluminate formation in limestone filler-blended cements. Cem. Concr. Res. 31, 853–859

Morandeau, A., Thiéry, M., Dangla, P., 2014. Investigation of the carbonation mechanism of CH and C-S-H in terms of kinetics, microstructure changes and moisture properties. Cem. Concr. Res. 56, 153–170. https://doi.org/10.1016/j.cemconres.2013.11.015

MPA: UK Concrete and cement industry roadmap to beyond net zero (2020). Mineral Product Association

Myers, R.J., L'Hôpital, E., Provis, J.L., Lothenbach, B., 2015. Effect of temperature and aluminium on calcium (alumino)silicate hydrate chemistry under equilibrium conditions. Cem. Concr. Res. 68, 83–93. https://doi.org/10.1016/j.cemconres.2014.10.015

Natkunarajah, K., Masilamani, K., Maheswaran, S., Lothenbach, B., Amarasinghe, D.A.S., Attygalle, D., 2022. Analysis of the trend of pH changes of concrete pore solution during the hydration by various analytical methods. Cem. Concr. Res. 156, 106780. https://doi.org/10.1016/j.cemconres.2022.106780

Pandey, S., Srivastava, V.C., Kumar, V., 2021. Comparative thermodynamic analysis of CO_2 based dimethyl carbonate synthesis routes. Can. J. Chem. Eng. 99, 467–478. https://doi.org/10.1002/cjce.23893

Pham, B.T., Wang, M., Luo, S., Ling, T.-C., 2024. Addressing workability issue and performance of CO2-mixed cement pastes. Constr. Build. Mater. 436, 136800. https://doi.org/10.1016/j.conbuildmat.2024.136800

Wu, B., Ye, G., 2017. Development of porosity of cement paste blended with supplementary cementitious materials after carbonation. Constr. Build. Mater. 145, 52-61. https://dx.doi.org/10.1016/j.conbuildmat.2017.03.176

Ramli, N.A.A., Kusin, F.M., Molahid, V.L.M., 2021. Influencing Factors of the Mineral Carbonation Process of Iron Ore Mining Waste in Sequestering Atmospheric Carbon Dioxide. Sustainability 13, 1866. https://doi.org/10.3390/su13041866

Rashid, S., Singh, M., 2023. An Investigation on Carbon Dioxide Incorporated Sustainable Ready-Mix Concrete Using OPC and PPC. Arab. J. Sci. Eng. 48, 14213–14236. https://doi.org/10.1007/s13369-023-08106-y

Ren, S., Huang, G., Zhang, W., Sha, X., Liu, G., Lin, R.-S., Chen, L., 2024. Enhancing cement-based materials hydration and carbonation efficiency with pre-carbonated lime mud. J. CO2 Util. 88, 102928. https://doi.org/10.1016/j.jcou.2024.102928

Richardson, I.G., 1999. The nature of C-S-H in hardened cements. Cem. Concr. Res. 29, 1131–1147. https://doi.org/10.1016/S0008-8846(99)00168-4

Richardson, J.M., Biernacki, J.J., Stutzman, P.E., Bentz, D.P., 2002. Stoichiometry of Slag Hydration with Calcium Hydroxide. J. Am. Ceram. Soc. 85, 947–953. https://doi.org/10.1111/j.1151-2916.2002.tb00197.x

Scrivener, K., Martirena, F., Bishnoi, S., Maity, S., 2018a. Calcined clay limestone cements (LC3). Cem. Concr. Res. 114, 49–56. https://doi.org/10.1016/j.cemconres.2017.08.017

Scrivener, K., Snellings, R., Lothenbach, B. (Eds.), 2018. A Practical Guide to Microstructural Analysis of Cementitious Materials, 0 ed. CRC Press. https://doi.org/10.1201/b19074

Scrivener, K.L., Juilland, P., Monteiro, P.J.M., 2015. Advances in understanding hydration of Portland cement. Cem. Concr. Res. 78, 38–56. https://doi.org/10.1016/j.cemconres.2015.05.025

Sharma, R., Kim, H., Lee, N.K., Park, J.-J., Jang, J.G., 2023. Microstructural characteristics and CO2 uptake of calcium sulfoaluminate cement by carbonation curing at different water-to-cement ratios. Cem. Concr. Res. 163, 107012. https://doi.org/10.1016/j.cemconres.2022.107012

Sikament LA45, Product Data sheet, Sika

Srivastava, A., Kumar, R., Lakhani, R., 2021. Low Energy/Low Carbon Eco-Cementitious Binders as an Alternative to Ordinary Portland Cement, in: Hussain, C.M., Di Sia, P. (Eds.), Handbook of Smart Materials, Technologies, and Devices. Springer International Publishing, Cham, pp. 1–23. https://doi.org/10.1007/978-3-030-58675-1_143-1

Stefaniuk, D., Hajduczek, M., Weaver, J.C., Ulm, F.J., Masic, A., 2023. Cementing CO_2 into C-S-H: A step toward concrete carbon neutrality. PNAS Nexus 2, pgad052. https://doi.org/10.1093/pnasnexus/pgad052

Suescum-Morales, D., Fernández-Rodríguez, J.M., Jiménez, J.R., 2022. Use of carbonated water to improve the mechanical properties and reduce the carbon footprint of cement-based materials with recycled aggregates. J. CO_2 Util. 57, 101886. https://doi.org/10.1016/j.jcou.2022.101886

Sun, J., Zunino, F., Scrivener, K., 2024. Hydration and phase assemblage of limestone calcined clay cements (LC3) with clinker content below 50 %. Cem. Concr. Res. 177, 107417. https://doi.org/10.1016/j.cemconres.2023.107417

Syamsunur, D., Wei, L., Ahmed Memon, Z., Surol, S., Md Yusoff, N.I., 2022. Concrete Performance Attenuation of Mix Nano-SiO_2 and Nano-$CaCO_3$ under High Temperature: A Comprehensive Review. Materials 15, 7073. https://doi.org/10.3390/ma15207073

Tajuelo Rodriguez, E., Garbev, K., Merz, D., Black, L., Richardson, I.G., 2017. Thermal stability of C-S-H phases and applicability of Richardson and Groves' and Richardson C-(A)-S-H(I) models to synthetic C-S-H. Cem. Concr. Res. 93, 45–56. https://doi.org/10.1016/j.cemconres.2016.12.005

Tompkins, D.C., Stewart, D.I., Graham, J.T., Burke, I.T., 2025. Dissolution kinetics of crushed concrete waste: Effect of pH on leaching behaviour. Waste Manag. 206, 115096. https://doi.org/10.1016/j.wasman.2025.115096

Niven, R., Monkman, G.S., Forgeron, D.P., 2016. US Patent no: 9492945, Carbon cure Technologies

Von Greve-Dierfeld, S., Lothenbach, B., Vollpracht, A., Wu, B., Huet, B., Andrade, C., Medina, C., Thiel, C., Gruyaert, E., Vanoutrive, H., Saéz Del Bosque, I.F., Ignjatovic, I., Elsen, J., Provis, J.L., Scrivener, K., Thienel, K.-C., Sideris, K., Zajac, M., Alderete, N., Cizer, Ö., Van Den Heede, P., Hooton, R.D., Kamali-Bernard, S., Bernal, S.A., Zhao, Z., Shi, Z., De Belie, N., 2020a. Understanding the carbonation of concrete with supplementary cementitious materials: a critical review by RILEM TC 281-CCC. Mater. Struct. 53, 136. https://doi.org/10.1617/s11527-020-01558-w

Wagner, D., Bellmann, F., Neubauer, J., 2023. Investigations on the effect of alkalis on C-S-H growth rates and their impact on early C3S hydration rates. Cem. Concr. Res. 173, 107268. https://doi.org/10.1016/j.cemconres.2023.107268

Wang, D., Zhang, Q., Feng, Y., Chen, Q., Xiao, C., Li, H., Xiang, Y., Qi, C., 2022. Hydration and Mechanical Properties of Blended Cement with Copper Slag Pretreated by Thermochemical Modification. Materials 15, 3477. https://doi.org/10.3390/ma15103477

Wang, W.-C., Lee, M.-G., Deng, J.-L., Wang, Y.-C., Chuo, S.-F., Pei-Chi, H., Jen-Wei, S., 2024. Study on carbon sequestration and CO2 mixing of fresh cement mortar. Case Stud. Constr. Mater. 21, e03813. https://doi.org/10.1016/j.cscm.2024.e03813

Durability index testing procedure manual Part 3: Standard procedure for water sorptivity and porosity test. University of Cape Town

Winnefeld, F., Leemann, A., German, A., Lothenbach, B., 2022. CO_2 storage in cement and concrete by mineral carbonation 8 p. https://doi.org/10.3929/ETHZ-B-000579767

Winnefeld, F., Zingg, A., Holzer, L., Pakusch, J., Becker, S., 2019. The ettringite – superplasticizer interaction and its impact on the ettringite distribution in cement suspensions.

Xia, Y., Liu, M., Zhao, Y., Chi, X., Guo, J., Du, D., Du, J., 2023. Hydration of ternary blended cements with sewage sludge ash and limestone: Hydration mechanism and phase

assemblage. Constr. Build. Mater. 375, 130868. https://doi.org/10.1016/j.conbuildmat.2023.130868
Xin, M., Zhang, L., Ge, S., Cheng, X., 2017. Effects of glass fiber modified with calcium silicate hydrate (C-S-H(I)) reinforced cement. IOP Conf. Ser. Mater. Sci. Eng. 182, 012040. https://doi.org/10.1088/1757-899X/182/1/012040
You, X., Hu, X., He, P., Liu, J., Shi, C., 2022. A review on the modelling of carbonation of hardened and fresh cement-based materials. Cem. Concr. Compos. 125, 104315. https://doi.org/10.1016/j.cemconcomp.2021.104315
Zajac, M., Irbe, L., Bullerjahn, F., Hilbig, H., Ben Haha, M., 2022b. Mechanisms of carbonation hydration hardening in Portland cements. Cem. Concr. Res. 152, 106687. https://doi.org/10.1016/j.cemconres.2021.106687
Zhang, Y., Çopuroğlu, O., 2022. The role of hydrotalcite-like phase and monosulfate in slag cement paste during atmospheric and accelerated carbonation. Cem. Concr. Compos. 132, 104642. https://doi.org/10.1016/j.cemconcomp.2022.104642
Zhang, Z., Xiong, Y., Jia, Z., Cao, R., Gao, Y., Maruyama, I., Zhang, Y., Wang, W., 2024. In-situ wet carbonation of steel slag powder paste made with carbonated water: Interaction mechanism between carbonation and hydration. Cem. Concr. Compos. 152, 105677. https://doi.org/10.1016/j.cemconcomp.2024.105677
Zheng, L., Nico, P., Spycher, N., Domen, J., Credoz, A., 2021. Potential impacts of CO_2 leakage on groundwater quality of overlying aquifer at geological carbon sequestration sites: A review and a proposed assessment procedure. Greenh. Gases Sci. Technol. 11, 1134–1166. https://doi.org/10.1002/ghg.2104
Zhuang, S., Wang, Q., Luo, T., 2022. Effect of C12A7 in steel slag on the early-age hydration of cement. Cem. Concr. Res. 162, 107010. https://doi.org/10.1016/j.cemconres.2022.107010
Zunino, F., Scrivener, K., 2025. Hydration and strength development of low-clinker (<50 %) factor limestone calcined clay cements (LC3): A comparative study with natural pozzolans. Constr. Build. Mater. 499, 144075. https://doi.org/10.1016/j.conbuildmat.2025.144075
Zunino, F., Scrivener, K., 2022. Insights on the role of alumina content and the filler effect on the sulfate requirement of PC and blended cements. Cem. Concr. Res. 160, 106929. https://doi.org/10.1016/j.cemconres.2022.106929